Advancements of combustion technologies in the ammonia-fuelled engines

Meng-Choung Chiong[a,*], Cheng Tung Chong[b], Jo-Han Ng[c], Syed Mashruk[d], William Woei Fong Chong[e,f], Guo Ren Mong[g], Agustin Valera-Medina[d]

[a] Department of Mechanical Engineering, Faculty of Engineering, Technology & Built Environment, UCSI University, 56000 Kuala Lumpur, Malaysia.
[b] China-UK Low Carbon College, Shanghai Jiao Tong University, Lingang, Shanghai 201306, China.
[c] Faculty of Engineering and Physical Sciences, University of Southampton Malaysia (UoSM), 79200 Iskandar Puteri, Johor, Malaysia.
[d] College of Physical Sciences and Engineering, Cardiff University, Wales, United Kingdom.
[e] School of Mechanical Engineering, Faculty of Engineering, Universiti Teknologi Malaysia, 81310 Skudai, Johor, Malaysia.
[f] Automotive Development Centre (ADC), Universiti Teknologi Malaysia, 81310 Skudai, Johor, Malaysia.
[g] School of Energy and Chemical Engineering, Xiamen University Malaysia, 43900 Sepang, Selangor, Malaysia

Abstract

This paper reviews the progress of ammonia (NH_3) combustion technologies in Spark Ignited (SI) engine, Compression Ignited (CI) engine, and Gas Turbine (GT). Hydrogen (H_2) was typically used to assist NH_3 combustion in the SI engine. NH_3 dissociator and the separate H_2 supply system are two common methods used to introduce H_2 into the engine. Elevating H_2 mass fraction to >10% is needed to acquire comparable engine performances with that of neat gasoline. Further increase in H_2 mass fraction may require engine parameters optimisation, due to the reduction in turbulent flame speed. Aqueous ammonia was one of the resolutions to enhance CI engine performances. Despite improving engine efficiency and emissions performance, aqueous ammonia could possibly lead to higher noise levels because of the increased ignition delay. Optimising the mass flow and timing of multiple injections is a more promising solution for reducing N_2-based emissions while also improving CI engine heat release rate (HRR). Partially premixed combustion has recently gained much attention in NH_3 gas turbine research, owing to its capability of extending the Lean Blowoff (LBO) limit of the flame to equivalence ratio (φ)~0.4. N_2-based emissions were reduced substantially when combustion takes place at φ~0.4. In all, NH_3 offers a practical opportunity for sustainable power production via internal combustion engines. The inferior NH_3 combustion and emissions performances can be improved through ground-breaking combustion technologies in these engines.

Keywords: Ammonia; gas turbine; internal combustion engine; partially premixed combustion; renewable energy

1.0 Introduction

Hydrocarbon fuels remain as the primary energy source nowadays to power our economy and daily life [1,2]. Nonetheless, this is achieved at the expense of environmental sustainability where the combustion of hydrocarbon fuels such as coal, crude oil, and natural gas undesirably elevates carbon dioxide (CO_2) concentration in the atmosphere, intensifying global warming effects as a result. The CO_2 concentration has increased linearly by a factor of 1.1 since 2006 [3]. Consequently, disastrous global warming effects are also escalating at a terrifying rate. The years of 2016 and 2020 have been the hottest years since record-keeping began, with a global surface temperature that climbed 1.02 °C above average temperatures recorded between 1951-1980 (Fig. 1) [3]. Owing to the additional water from melting ice caps, the global sea level has rose by 8" since 1880, posing direct threats to the coastal cities [3].

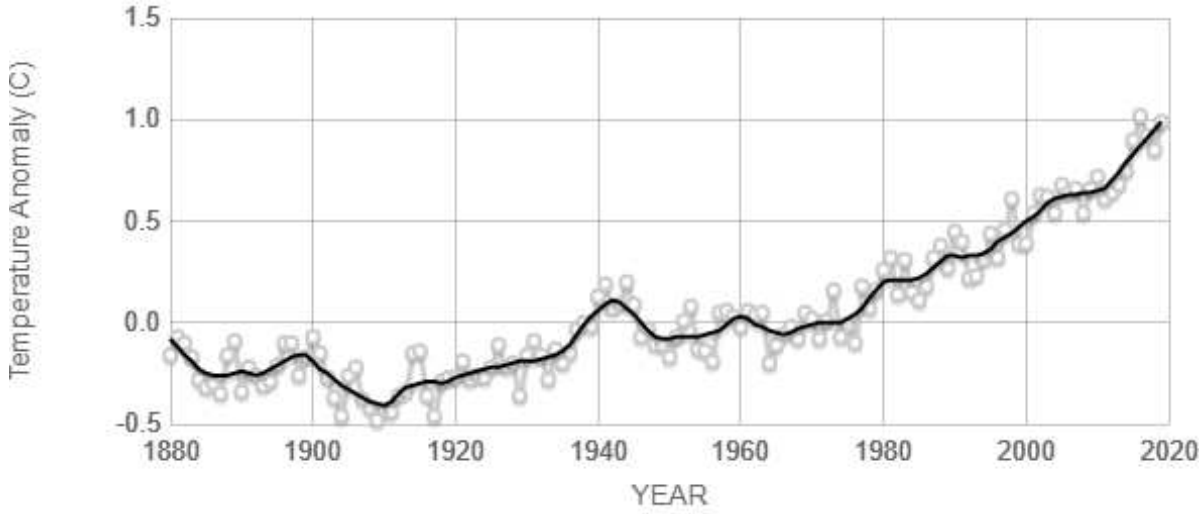

Fig. 1 Global land-ocean temperature index (reprint from [3])

In 2018, the United Nations Intergovernmental Panel on Climate Change (IPCC) gave a noteworthy alert that global carbon pollution must be reduced by half within the next 10 years to avoid causing irreversible damages to our living environment. Therefore, global decarbonisation efforts have become more imminent than ever to minimise carbon-based fuels

consumptions. The IPCC initiative inherently unlocks carbon-free energy sources such as Hydrogen (H_2) and Ammonia (NH_3) as viable replacements for conventional hydrocarbon fuels. Although H_2 is an attractive carbon-free energy source, its storage is difficult and more expensive due to either its refrigeration at cryogenic conditions or high compression (~350-700 bar), parameters needed to attain competitive energy density, as illustrated in Fig. 2 [4]. Ammonia, on the other hand, exhibits higher energy density than H_2 with a substantially lower compression pressure of 10 bar (chilling to -35 °C) [4].

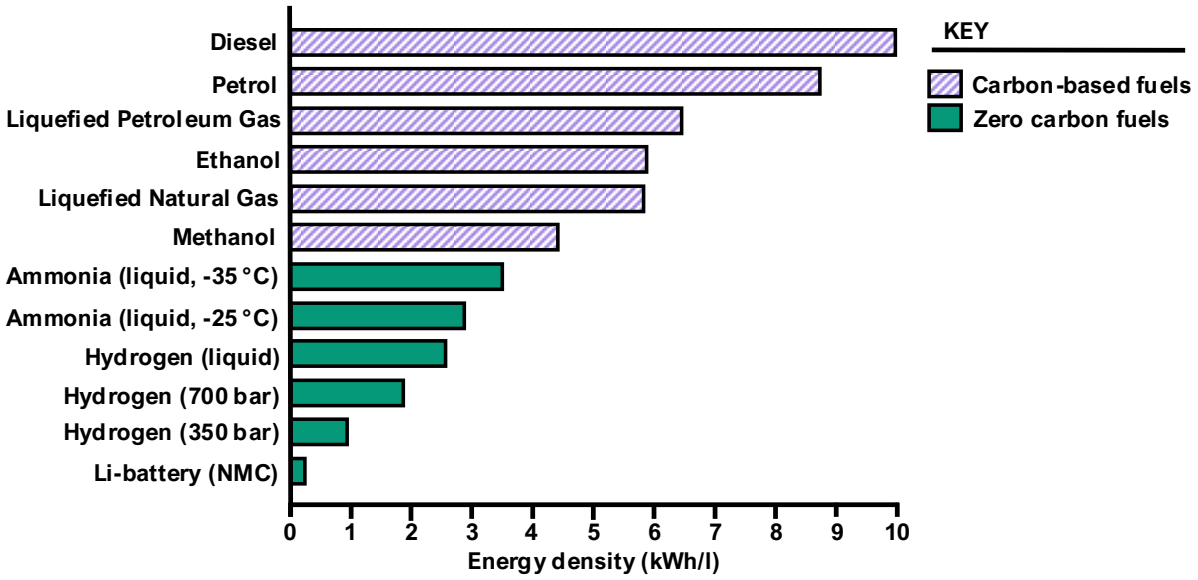

Fig. 2 The energy density of a range of fuel options (adapted from [4])

Ammonia is primarily produced via the well-established Haber-Bosch process that utilises iron-based catalyst to combine nitrogen (N_2) and H_2 under high pressure ~300 bar and temperature ~400 °C through the main reaction $N_2 + H_2 \leftrightarrow 2NH_3$ [5]. For the production of green ammonia, N_2 and H_2 need to be acquired via electrolysis of water and air separation, respectively. For over a century, ammonia has been extensively used as a fertiliser where it has played a critical role in ensuring that our world is fed adequately. Ammonia has also been used as the refrigerant in cold storage and large-scale air-conditioning systems since the 1930s. Meanwhile, ammonia is also the key chemical additive for selective catalytic reduction (SCR)

in automotive systems. Concurrently, ammonia was a momentary option for transportation fuel during the energy crisis in the 1960-1970s [6]. Since the last decade, intensified global decarbonisation campaigns have shortlisted NH_3 as an alternative energy source again, expanding its application into electricity generation and transportation fuel where direct combustion is involved [4].

Like many alternative fuels with inferior physicochemical properties, it has been reported that significantly higher ignition energy was needed to ignite ammonia when compared with fossil fuels, owing to the lower ammonia flammability [7,8]. The minimum ignition energy for the ammonia/air mixture at near stoichiometric was higher than the propane/air mixture by a factor of ~21.5 [8]. Furthermore, the flammability limit of ammonia is also noticeably narrower than methane (CH_4) and hydrogen. The NH_3 can only operate within equivalence ratios (φ) between 0.63-1.40, while methane and H_2 can operate in a wider range of $0.5< \varphi <1.7$ and $0.1< \varphi <7.1$, respectively [9]. Laminar flame speed (S_L) for NH_3 is also significantly lower than those of H_2 and CH_4 [9,10]. S_L for NH_3/air was ~7 cm/s at stoichiometric conditions, whereas stoichiometric S_L for CH_4/air and H_2/air were ~37 cm/s and ~291 cm/s, respectively [9,10]. A study by Li et al. [11] showed that S_L for NH_3/CH_4 increased by a factor of ~4 when NH_3 concentration in the fuel mixture reduced by ~26.7 vol.%. Emission-wise, fuel N_2 has a predominant effect on Nitric Oxide (NO) formation in NH_3 combustion. Owing to the low N_2 reactivity, flame thickness for NH_3 is an order of magnitude larger than methane at stoichiometric conditions. In contrast to methane, NO increased drastically within the thickened reaction zone for NH_3 combustion rather than in the post-flame zone, indicating the predominant fuel-NO pathway than thermal NO route in NH_3 combustion systems [9,12].

Overall, NH_3 exhibits lower reactivity than conventional carbon-based fuels, leading to unsatisfactory combustion and emissions performances [6,9]. These major drawbacks have

hindered its extensive use in current power generation industries. Due to its significantly different characteristics than carbon-based fuels, a recent review stressed that NH_3 combustion requires distinctively different strategies than that of hydrocarbon fuels [5]. Enhanced NH_3 combustion and emissions performances are of paramount importance to promote NH_3 as a cleaner solution for future power generation. Three types of internal combustion engines that are commonly used for power generations were chosen for this review, namely Spark Ignited (SI) engine, Compression Ignited (CI) engine, and Gas Turbine (GT).

It was reported that the annual reciprocal engine capacity installed around the globe was 49.6-56.5 GW during the years of 2013-2016 [13]. In the US, the capacity of reciprocal engines was below 9 MW before 2010. However, larger units with an output power of 16-19 MW have been deployed across the US since the last decade. The Denton Energy Center, located outside of Dallas, Texas, is the largest of these plants, with a total plant capacity of ~225 MW [14]. Similarly, gas turbine plants have been the method of choice for electricity generation in many developed countries since the invention of gas turbine combined cycles (GTCC) [2,15,16]. Gas turbines generated ~508.5 GW of electricity in January 2017 in the US and increased to ~543.6 GW in January 2021 [17]. Therefore, the increasing importance of reciprocating and gas turbine engines for power generation is evident, primarily because they can deliver incremental electricity easily with flexible operation. These units have become increasingly popular in areas with large shares of renewable electricity production because they can start and stop quickly and run at partial loads [14]. To date, various engine combustion strategies have been proposed and studied for ammonia blends. This paper critically reviews the development of ammonia combustion technologies in SI engine, CI engine, and GT.

2.0 Ammonia in Spark Ignition (SI) Engine

The combustion of neat gaseous NH_3 in an SI engine was examined by Cornelius et al. [18]. The liquid ammonia was vaporised into gaseous form and injected into the intake manifold to mix with intake air [18]. The start of ignition (SOI) for the NH_3 engine was advanced by ~100 °CA (degree Crank Angle) bTDC (before Top Dead Centre) to acquire stable engine operation. However, even with advanced SOI, the indicated thermal efficiency (ITE) of such an ammonia engine was ~12% lower than neat gasoline engines running at 2400 RPM [18]. Worse still, the NH_3 engine could only operate up to 2400 RPM [18]. It was reported that increased engine compression ratios (CR) from 9.4 (baseline) to 18 could extend engine operating speed to 4000 RPM under full throttle. Turbocharging the NH_3 SI engine with CR > 11.5 resulted in very similar engine output power with naturally aspired (NA) gasoline engines (CR 9.4). The study by Cornelius et al. [18] ascertained that NH_3 engine stability can be enhanced by optimising the engine parameters, lessening the concerns whether the SI engine cannot give satisfactory performance when fuelled with neat NH_3 [19–21].

A more recent study on neat gaseous NH_3 SI engine was reported by Lhuillier et al. [22–24]. Like Cornelius et al. [18], gaseous ammonia was mixed with air in the intake plenum prior to entering the combustion chamber. It was shown that pure ammonia could attain stable SI engine operation (given by the coefficient of variation of the indicated mean effective pressure (COV_{IMEP}) < 3% [24]) for intake pressures (P_{in}) ≥ 1 bar and $0.9 < \phi < 1.1$ when SOI was advanced to ~40°CA bTDC to compensate for the slow NH_3 flame propagation. Nitrogen Oxide (NO_x) emission of neat ammonia engine increased by ~1000 ppm when P_{in} increased by 0.2 bar for $\phi \leq 1$. Furthermore, H_2 addition increased NO_x emission noticeably for all tested operating points [22–24]. The individual influences of engine parameters on NH_3 SI engine performances are shown in Fig. 3.

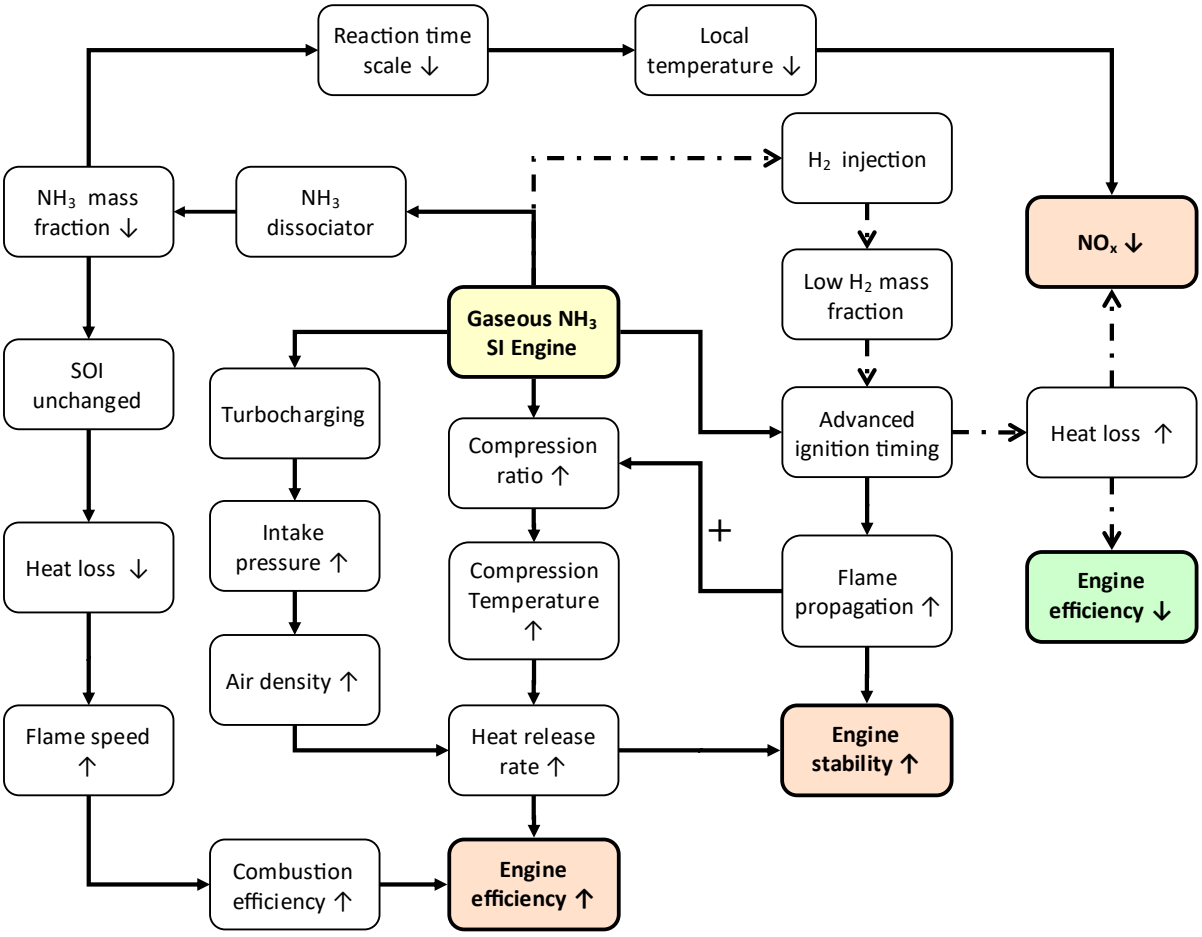

Fig. 3 SI engine parameters adjustments to accommodate gaseous NH_3 and NH_3/H_2 operations.

In addition to adjusting the engine operating parameters, NH_3 can be dissociated to produce in-situ hydrogen, thus increasing flame speed and combustion stability. Sawyer et al. [25] decomposed NH_3 into N_2 and H_2 by means of a "dissociator" that consisted of a stainless-steel chamber loosely filled with the catalyst and electrically heated by heater units. Up to 25°/o of the NH_3 was decomposed and the produced H_2 (5% vol.) was mixed with the remaining NH_3. The cylinder pressure for the Iso-Octane engine was lower than for the NH_3/H_2 engine by as many as ~100 psia for $\phi < 0.8$. Conversely, Starkman et al. [26] reported that IMEP of this NH_3/H_2 engine with CR 10 was ~40 psi lower than for the Iso-Octane engine at near stoichiometric combustion, leading to efficiencies twice lower than that of the Iso-Octane engine. Cornelius et al. [18] showed that H_2 addition from 0% to 3% extended NA-full throttle in the NH_3 engine's operational range from 2400 RPM to 4000 RPM at CR = 9.4. Moreover,

engine ITE was nearly identical with the gasoline engine from 2-4 horsepower (hp) engine output power with 2.5% H_2 addition.

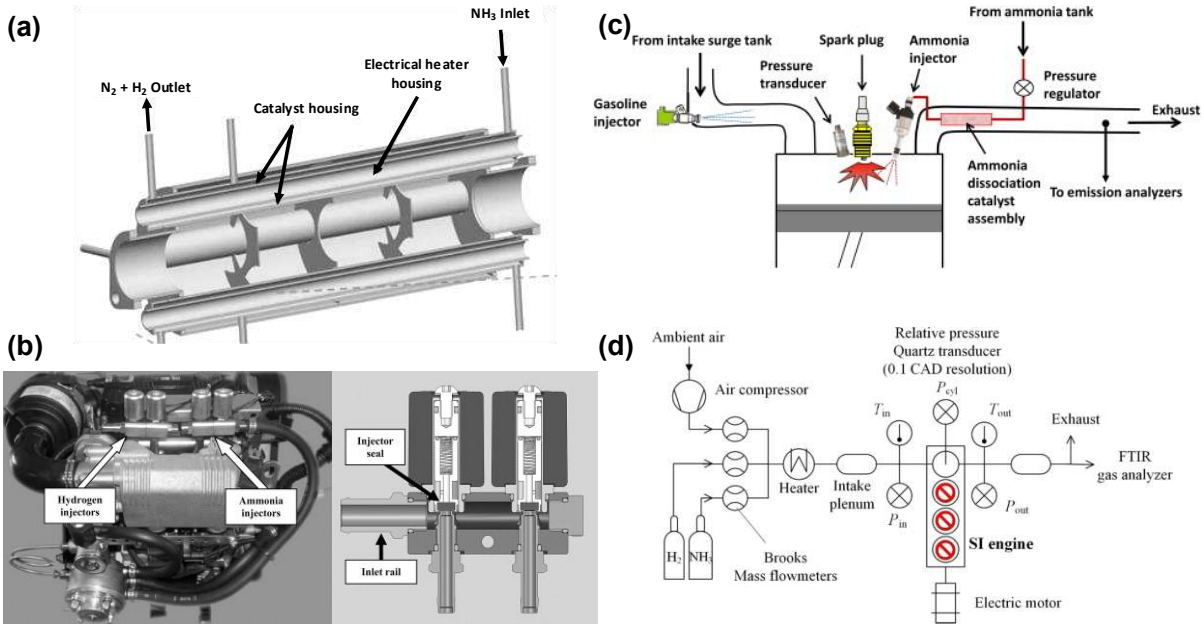

Fig. 4 (a) Catalytic cracker reactor for NH_3 dissociation, (b) Ammonia and Hydrogen injectors system, (c) Ammonia and Hydrogen direct injection system, (d) Ammonia and Hydrogen Port Fuel Injection (PFI) system (reprint from [24,27–29] with permission from Elsevier).

Ryu et al. [29] utilised hot exhaust gas to dissociate the NH_3. Dissociated NH_3 was injected into the combustion chamber and mixed with a gasoline/air mixture. Brake power for the engine with NH_3 dissociation was elevated by an average of ~0.2 kW when compared with that of gasoline/NH_3 engines without NH_3 dissociation. NO_x emission for the engine with NH_3 dissociation was lower than an engine without the NH_3 dissociation system by ~25 g/kWh. Furthermore, slip NH_3 and carbon monoxide (CO) emissions for the former were lowered by 2.5 g/kWh and 8 g/kWh, respectively. Frigo [27,30] developed a Hydrogen Generation System (HGS) for NH_3 dissociation, as depicted in Fig. 4a. The main component of the HGS is a cracking reactor housing a ruthenium-based catalyst. It was shown that an NH_3/H_2 engine operating at 3000 RPM recorded nearly identical brake thermal efficiency (BTE ~28%) to that of a gasoline engine. While the BTE of gasoline engine started to fall below 28% when engine

speed >3000 RPM, BTE of ammonia/hydrogen engine remained at ~28%. NO_x emission from the ammonia/hydrogen engine was averaging 1000 ppm lower than the gasoline engine (Fig. 3).

The thermodynamics advantages of the liquid ammonia dissociation system were ascertained by Ezzat and Dincer [31,32]. It was demonstrated that the ammonia dissociator system increased engine output power as NH_3 mass fraction increased, although both the energy and exergy efficiencies declined undesirably. Exergy destruction due to irreversibility also increased as NH_3 mass fraction increased. As compared to vehicle systems that could be powered using fuel cells with NH_3, the dissociator vehicle elevated energy efficiencies by ~30% at maximum traction power of 118 kW. In another vehicle system proposed by Ezzat and Dincer, H_2 was produced onboard using ammonia electrolyte cell (AEC). A thermoelectric generator (TEG) was used for waste heat recovery from the SI engine. The overall energy and exergy efficiencies of the system were found to be 31.1% and 28.94%, respectively [31]. Overall, the NH_3 dissociator vehicle exhibited the highest energy and fuel efficiencies among the three systems examined.

Apart from dissociating the NH_3 into N_2 and H_2, another way of enabling a NH_3/H_2 engine can be by injecting the NH_3 and H_2 separately into the intake manifold of the SI engine. An electro-injector (Fig. 4b) was used for NH_3 and H_2 injection in an experimental engine. It was demonstrated that the BTE of NH_3/H_2 blending was 3-4% lower than the gasoline engine from 2500-5000 RPM [28,33]. Mørch et al. [34] also utilised separate NH_3 and H_2 injection methods. It was reported that blending ammonia with ~5 vol% hydrogen could still lead to a good power response [97]. By elevating the hydrogen to ~10 vol%, the engine ITE increased by 0.5% as compared to a neat gasoline engine [98]. Nonetheless, NO_x emissions of ~750 ppm were produced when hydrogen content was increased to ~20 vol%, thus suggesting the need for SCR at the exhaust gases under these conditions. Westlye et al. [35] found that NO_x

emissions of an NH_3/H_2 engine increased by ~2000 ppm as fuel injection timing was advanced by 40°CA for $\lambda > 1$. NO_2 increased by ~100 ppm while N_2O decreased by 50 ppm. Slip NH_3 remained unchanged as SOI was advanced to 40°CA bTDC. Moreover, it was also found that NO, NO_2, and slip NH_3 increased by 1000 ppm, 25 ppm, 1500 ppm, respectively as CR increased from 7 to 15 for $\lambda > 1$ operation. Another development that used separate injection was presented by Cardiff University through the development of their Green Ammonia demonstrator at the Rutherford Appleton Laboratory. The results showed that an injection of 30% (vol) hydrogen in an ammonia mixture could enable the replacement of methane for production of power up to 16kW at 1,500 RPM. Although NOx emissions were below 20ppm, it was observed that the combustion was still inefficient, thus requiring further development in terms of timing, equivalence ratio and injection strategy.

As shown in Fig. 3, Table 1, and Table 2, the use of NH_3 dissociation systems generally leads to higher engine efficiency than the gasoline engine. This is presumably due to the substantial reduction in NH_3 mass fraction that elevates the flame speed and combustion efficiency (Fig. 3). For a separate H_2 supply system, spark ignition timing must be retarded by another 10-15 °CA (compared to a gasoline engine) to ensure stable engine operation, thus resulting in higher heat loss and less residual expansion than gasoline engines [28]. It is expected that the separate H_2 supply system can deliver comparable engine performances with the NH_3 dissociation system if the H_2 mass fraction is increased to ~11% (like that of the NH_3 dissociation system). Emission-wise, NH_3 dissociation technology led to considerable NO_x reduction when compared with the gasoline engine, seemingly due to predominant H_2 combustion in the engine (Fig. 3). For a separate H_2 supply system, advanced SOI was required to reduce NO_x emission [35]. Owing to the substantial heat loss, thermal NO was reduced in the SI engine that employed a separate H_2 supply system.

In addition to NH_3 dissociation and separate H_2 supply, disputes also arise among directly injecting (DI) the NH_3 mixture into the combustion chamber (Fig. 4c) and PFI (Fig. 4d). To date, there are no systematic comparisons between these two types of fuel injection systems for the NH_3 SI engine yet. Only Ryu et al. [29,36] had reported their results on NH_3 direct-injection engines when blended with gasoline [29,36]. In contrast, studies that utilised the PFI technique did not blend the dissociated NH_3 with gasoline [24,28]. Hence, decent comparisons between both fuel induction techniques are not possible. As compared to a neat gasoline engine, the fuel efficiency of DI gasoline/NH_3/H_2 engine was lowered by ~10 MJ/kWh as compared to gasoline/NH_3 SI engines without a dissociation system [29,36], despite higher engine power was generated by the latter. Ammonia injection for ~22 ms was required for the DI gasoline/NH_3/H_2 engine to achieve similar fuel efficiency with a neat gasoline engine [29,36]. No direct emissions comparison between the DI gasoline/NH_3/H_2 engine and the neat gasoline engine was performed [29]. For the PFI engine, the thermal efficiency of the NH_3/H_2 is also lower than the neat gasoline engine [24,28]. Nonetheless, no direct emission assessment between NH_3/H_2 and the neat gasoline engine was performed [24,28]. Although reasonable comparison cannot be performed, it is expected that the fuel mixture in the DI NH_3 engine would be heterogeneous and the combustion would be predominantly non-premixed, owing that the gasoline/air was not mixed with NH_3/H_2 fuel spray before entering the combustion chamber. In PFI injection, however, fuel mixture and air are mixed prior to entering the combustion chamber. Hence, the reaction time scale is likely to be shorter and the combustion mode is primarily premixed.

259 Table 1 Comparison of NH_3/H_2 SI engine using NH_3 dissociator.

Tested Fuel	Baseline	Operating Conditions	Engine Performances	Emissions	References
NH_3/H_2	Iso-Octane	• Bore/Stroke = 0.72 • 25% of NH_3 dissociated into H_2 (~5%) & N_2. • 1800 RPM, CR = 10	• P_{cyl} ↑ by ~100 psia for ϕ < 0.8.	• NO ↑ by a factor of 1.5 (ϕ < 1)	Sawyer et al. [25]
NH_3/H_2	Iso-Octane	• 25% of NH_3 dissociated into H_2 (~5%) & N_2. • 1800 RPM, CR = 10	• Peak IMEP ↓ by ~50 psia (ϕ < 1) • Indicated Specific Fuel Consumption (ISFC) ↑ ~0.5 lbs/hp hr	• NO ↑ by a factor of 1.5 (ϕ < 1)	Starkman et al. [26]
NH_3/H_2	Gasoline	• Displacement = 442 cm^3 • Bore/Stroke = 1.12 • Part of NH_3 decomposed to produce ~2.5 wt.% H_2 • CR = 9.4, 1600 RPM	• ITE ↓ without H_2 addition • ITE ≈ as H_2 increased by ~3 vol.%. • BP ↑ by 8 hp as H_2 increased by ~3 vol.%.	-	Cornelius et al. [18]
NH_3/H_2	Gasoline	• Displacement = 505 cm^3 • Bore/Stroke = 1.16 • Full throttle, λ = 1 • $\dot{m}_{H2}$ = 1.38 Nm^3h^{-1} • $\dot{m}_{NH3}$ = 7-7.4 Nm^3h^{-1} • 2500-3500 RPM	• BTE ↓ 3% (2500 RPM) • BTE ↑ 1.5% (3500 RPM)	• NO_x ↓ ~1000 ppm. • High load NO_x > half load NO_x by ~200 ppm	Frigo [27,30]
Gasoline/ NH_3/H_2	Gasoline/NH_3	• Displacement = 611 cm^3 • Bore/Stroke = 0.72 • 1800 RPM, CR = 10 • $\dot{m}_{gasoline}$ = 27.5 g/min • NH_3 injected 270-370 bTDC • $\dot{m}_{ammonia}$ = 3.75-13.85 g/min	• BP ↑ ~0.2 kW • Brake Specific Energy Consumption (BSEC) ↓ ~5 MJ/kWh	• NO_x ↓ ~25 g/kWh ($\dot{m}_{ammonia}$ = 7.2 g/min) • NH_3 slip ↓ 83%. ($\dot{m}_{ammonia}$ = 7.2 g/min)	Ryu et al. [29]

Table 2 Comparison of NH_3/H_2 SI engine using separate H_2 supply.

Tested Fuel	Baseline	Operating Conditions	Engine Performances	Emissions	References
NH_3/H_2	Gasoline	• Displacement = 505 cm^3 • Bore/Stroke = 1.16 • 2500-5000 RPM • $\lambda = 1$ • CR = 10.7 • Full load • H_2 to NH_3 energy ratio: 6-8% (Full load)	• BTE ↓ by ~ 2.5% regardless of engine speed. • BP ↓ by ~ 3kW (3500 RPM)	• Full load NO_x ↓ by 1000 ppm against half load.	Frigo & Gentili [28,33]
NH_3/H_2	Gasoline	• Displacement = 612.5 cm^3 • Bore/Stroke = 0.72 • 1200 RPM • $\lambda > 1$ • H_2/NH_3 volume ratio: 10/90	• ITE ↑ by 0.5% as CR ↑ by 2.6.	• NO_x emission was 5500 ppm when H_2 vol% was 70% (CR = 8.9, λ = 1.3-1.4, H_2/NH_3 volume ratio = 70/30)	Mørch et al. [34]
NH_3/H_2	Gasoline	• Displacement = 612.5 cm^3 • 1000 RPM • λ = 1-1.4 • CR = 7-15 • Full throttle • H_2/NH_3 volume ratio: 20/80	-	• NO ↓ 1500 ppm as SOI advanced to 30 °CA bTDC. • NO_2 ↑ by ~100 ppm, N_2O ↓ by ~50 ppm as SOI advanced by 40 °CA.	Westlye et al. [35]

As depicted, mixing the ammonia with other fuels is a convenient way of enhancing its reactivity [37,38]. Thus, aside from neat NH_3 and NH_3/H_2 SI engines, Grannell et al. [19–21] established a gasoline/NH_3 blending map for SI engines. Engine operating parameters such as speed, load, and CR were considered to determine the optimum gasoline/NH_3 blending ratio that would deliver satisfactory engine performances. The authors concluded that no single, constant ratio of gasoline/NH_3 works appropriately for every engine operating condition. Thus, it was suggested that gasoline and ammonia should be stored separately and blended separately based on different engine operating conditions. However, Ryu et al. [29] showed in a later study that a gasoline/NH_3 ratio of 2-7.3 would yield satisfactory engine stability and performances from 0.6-2.75 kW engine output power. Oxygenated fuel addition was another approach to improving NH_3 SI engine performance. Haputhanthri et al. [39–42] blended the NH_3 with methanol/gasoline or ethanol/gasoline in 10%-20% volumetric ratio, thus increasing engine brake torque by approximately 10 Nm when the engine speed was > 3500 RPM. When the methanol volumetric ratio increased to 30%, a marginal increase in brake torque could be observed at engine speeds between 2000-2500 RPM. Ammonia-rich fuels with up to 20% of ethanol perform better than baseline fuel, especially at higher engine speeds [39–42].

H_2 is notably the most used additives for improving the combustion performances of NH_3 SI engines. However, there are also potential drawbacks in adding H_2 into the NH_3 SI engine. As shown in Fig. 5, H_2 addition elevated the peak heat release rate (HRR) by ~50% as its volume fraction increased by 15% [43], due to the increased turbulence flame velocity by about 50% that leads to shorter combustion duration (by ~15 °CA) and reduced heat loss [43]. Nonetheless, excessive H_2 addition (volume fraction > 10%) in NH_3 SI engine operation pulled the mixture effective Lewis number (Le) below 0.9, owing to the aggravated preferential diffusion effects between both reactants [43]. Flame stretching increased by a factor of 2 as Le falls below 0.9, promoting the local flame extinction and wrinkling. Although these did not

reduce the peak HRR, turbulent flame speed declined by ~16.7% [43]. In a practical engine test, Frigo et al. [27,30] showed that for H_2 mass fraction of ~22%, an engine speed of at least 3000 RPM is needed to ensure that the NH_3/H_2 engine efficiency remains competitive with that of the neat gasoline engine. Efficiency for the NH_3/H_2 engine declined drastically as engine speed fell below 3000 RPM.

Furthermore, increased N_2O emissions are another concern when using H_2 as an additive in the SI engine [44]. It was shown that N_2O emissions increased by ~50% as H_2 vol fraction by 12.5% was achieved under the fuel-lean combustion [44]. The drastic increase in N_2O is presumably due to the increased NO emission in fuel-lean operation that promotes N_2O formation via $NH + NO \rightarrow N_2O + H$. N_2O is nearly 300 times more potent than CO_2 [45]. Thus, releasing N_2O emission into the ambient air would have a tremendous impact on global warming, comprising a challenging task for the NH_3/H_2 SI engine. Another additive would be CH_4. As depicted in Fig. 5, the peak HRR of NH_3 premixed flame reduced by ~40% as CH_4 volume fraction increased by 15%. This was attributed to the combustion duration which increased by approximately 10 °CA as CH_4 volume fraction raised to 15%. In general, despite H_2 mass fraction ~10% resulted in promising engine performance improvement, engine parameters optimisation may have to be performed if H_2 mass fraction is to be increased further, due to the limitations of excessive H_2 addition shown in Fig. 5.

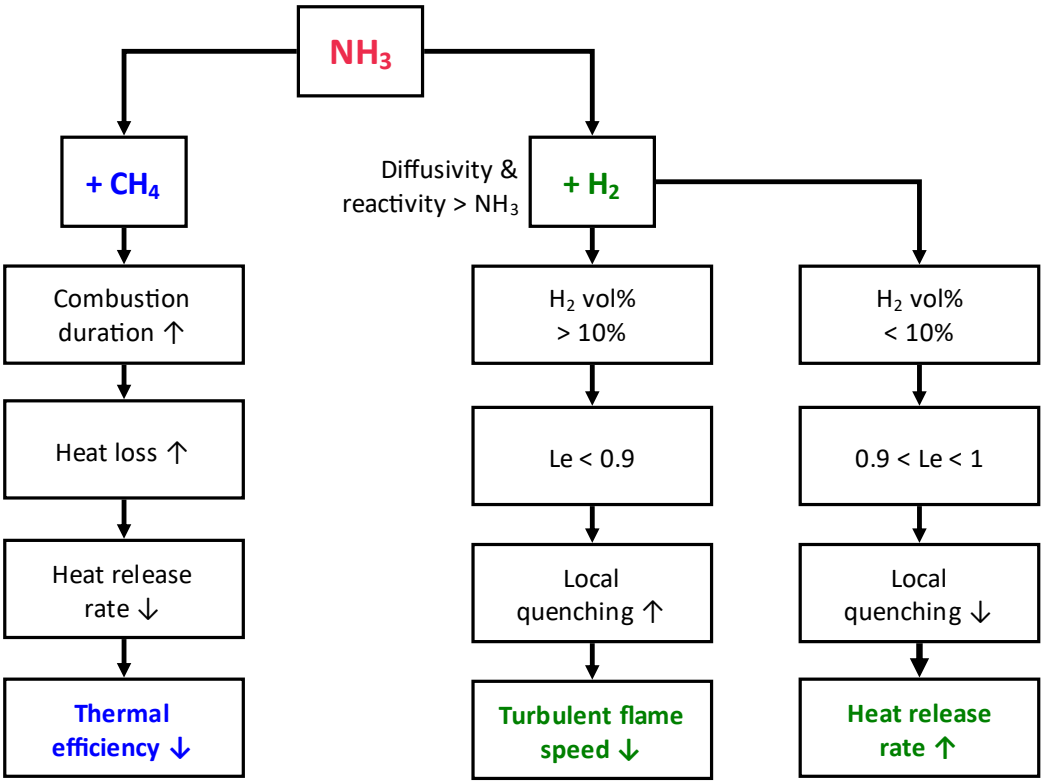

Fig. 5 Overview of CH_4 and H_2 as additive for NH_3 SI engine.

3.0 Ammonia in Compression Ignition (CI) Engine

The CI engine with inherently higher CR (14-25) and thermal efficiency (η: 45-55%) than the SI engine (CR: 8-12, η: 28-42%) is another type of piston machine commonly used for power generation. The annual installed capacity for CI engine is about an order of magnitude higher than that of SI engines [13]. Aside from the power generation industry, the shipping industry is another large fossil fuel user that consumes ~330 million metric tons of fuels annually [46]. Heavy Fuel Oil (HFO) with high level of sulphur is typically used to propel marine cargo vessels, contributing directly to the Sulphur Oxide (SO_x) emission following its combustion in engines [47]. The International Maritime Organization (IMO) imposed stricter regulations on ship fuel to ameliorate harmful SO_x emission by lowering the limit of sulphur content for operation in the open seas from 3.5 wt.% to 0.5wt.% [48]. This is expected to reduce annual SO_x emission by ~ 8.5 million metric tonnes [48]. As a result of these initiatives, several researchers and maritime companies have diverted their attention to ammonia-fuelled CI engines [49–53]. Combustion in the CI engine is different from that of the SI engine, since the CI engine combustion consists of four distinct stages (i.e. ignition delay, pre-mixed burning, mixing controlled combustion, and after burning) [54]. The presence of NH_3 affects the combustion process at each stage and influences the reaction at the subsequent stages as a result.

Lamas Galdo et al. [55] showed that NO_x emissions of a 6-cylinder ammonia/marine diesel oil (MDO) CI engine could be reduced up to 80% by retarding the fuel injection timing to 58.4 °CA aTDC (after Top Dead Centre). Lamas & Rodriguez [56] also reported that optimum NO_x reduction (~60%) for a H_2/diesel/NH_3 engine was achieved at 43.2 °CA aTDC. Nonetheless, ammonia slip was found to increase by 30 ppm when the injection was retarded to after the TDC [55]. Niki et al. [57–59] reported that peak cylinder pressure of NH_3/diesel engines augmented by 1 MPa as the fuel SOI advanced by 5 °CA (from 8 to 13 °CA bTDC). The engine HRR was raised by ~10 J/°CA following the rise in the cylinder pressure. Multiple

injection strategies were also examined for the NH_3 CI engine. Despite advanced pilot injection from 30 to 70 °CA bTDC reduced NH_3 slip by as much as ~2200 ppm, N_2O and NO_x emissions were found to increase by a factor of 4 and 1.7, respectively [57–59]. Moreover, the engine HRR reduced by ~40 J/°CA when pilot injection was advanced by 50 °CA. This is mainly due to the substantial heat loss when combustion started at the early stage of the compression stroke. Retarded post-injection from 10 to 30 °CA aTDC reduced engine HRR by ~10 J/°CA. Tay et al. [60,61] showed that HRR and peak cylinder pressure for a kerosene/diesel/NH_3 engine increased by 125 J/°CA and 25 bar, respectively, as SOI was advanced by 18.5 °CA from TDC. Kerosene resulted in higher primary peak heat release during the premixed combustion phase, owing to its lower CN and higher latent heat of vaporisation. The duration of combustion (DOC) generally decreased when SOI was advanced. The mixture ignition delay, however, increased exponentially when SOI was advanced, endowing longer fuel evaporation and mixing time scales. NO emissions increased by a factor of 5 when SOI advanced from -3.5 to -17.5 °CA bTDC.

Lee and Song [62] applied multiple injection methods to a neat NH_3 engine. It was demonstrated that when the mass fraction of the pilot fuel is less than or equal to the main injection, SOI of at least -12 °CA bTDC is required to elevate engine in-cylinder pressure to a competitive level of ~170 bar. Conversely, when the mass fraction for the pilot fuel is higher than that of the main injection, SOI could be retarded to -4 °CA bTDC before a noticeable cylinder pressure drop takes place. When compared with -8 °CA bTDC SOI, NO emissions were reduced up to a factor of 5 when SOI was retarded to -12 °CA bTDC, owing to the reduction in peak cylinder temperature. Lamas and Rodriguez [63] showed that parabolic fuel injection profiles resulted in the highest NO_x reduction (~75%) when compared with rectangular and triangle ammonia injection profiles (~65%) at 40 °CA aTDC. It was also shown that prolonged injection duration (10 °CA) resulted in poorer NO_x reduction [63]. As shown in

Fig. 6, retarded fuel injection led to drastic NO reduction, owing to the heat loss during the expansion stroke. However, it is expected that fuel efficiency will be declined due to the late fuel injection strategy. Conversely, advanced injection of 10-18 °CA bTDC is seemingly a more practical approach. Although NO_x and N_2O showed an increasing trend from 0-10 °CA bTDC injection [57], it was reported that further advances in fuel injection could reduce NO_x drastically [61].

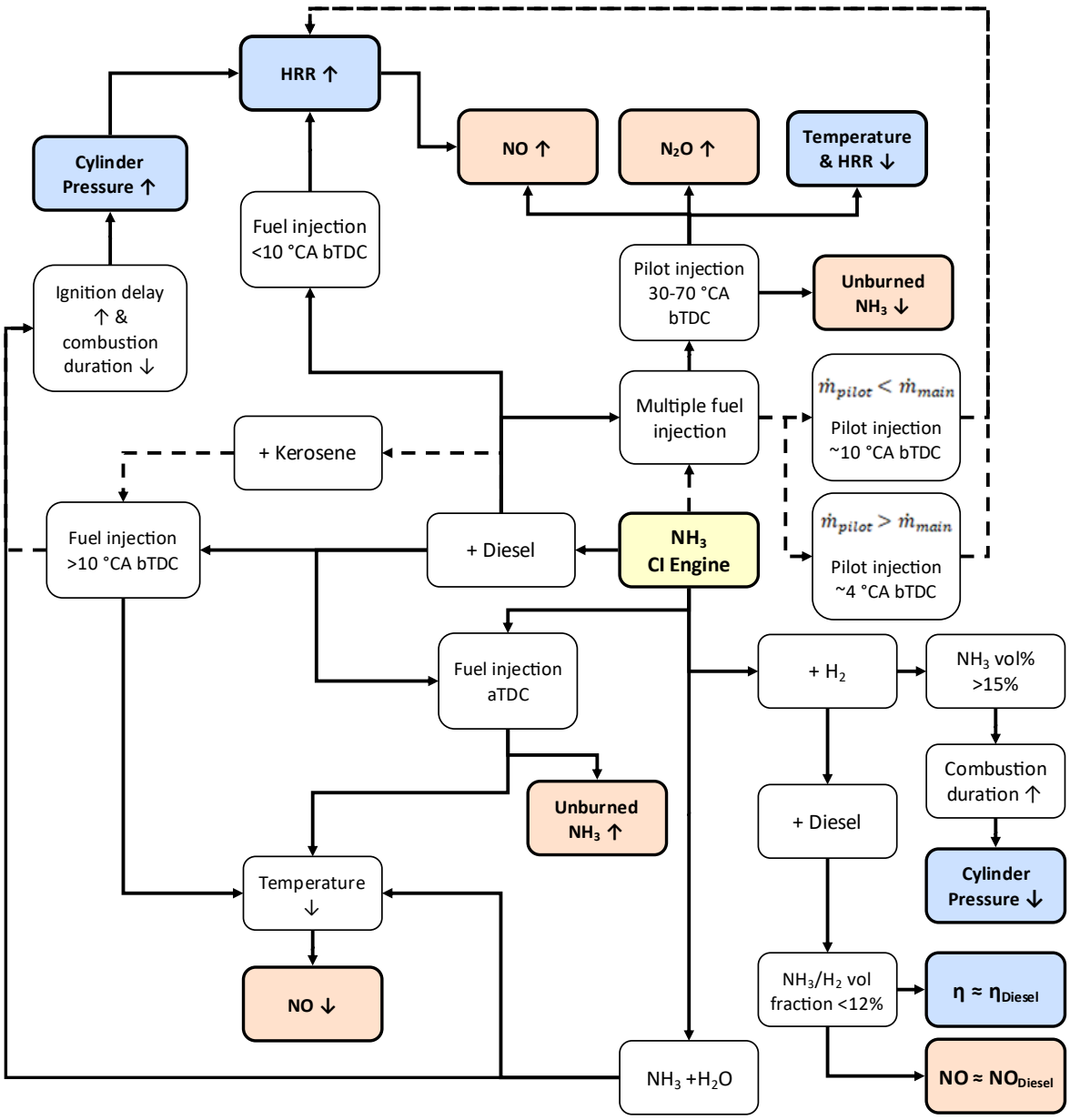

Fig. 6 CI engine parameters adjustments to accommodate NH_3 operations.

The idea of ammonia solution ($NH_3 + H_2O$) was investigated by Pyrc et al. [64] using a CI engine. Conventional diesel was chosen as the baseline. The engine heat release increased by 12 J/°CA at full load operation when fuelled with the water ammonia solution (WAS), owing to the increased ignition delay and prolonged combustion duration. As a result of the increased heat release, the engine BTE was found to increase by ~3%. Although WAS increased the engine COV_{IMEP} by about 0.3%, the overall COV_{IMEP} was lower than 5% (acceptable COV_{IMEP} [54]). NO_x emissions for the diesel/WAS engine were 520 ppm lower than diesel at full load, owing to the lower combustion temperature. Nonetheless, this resulted in 70 ppm higher Unburned Hydrocarbon (UHC) than the diesel engine. Schönborn [65] showed that aqueous ammonia was more difficult to ignite than neat ammonia in a CI engine. To ignite ammonia in an aqueous solution, a minimum CR of 27 was necessary for a typical CI engine operation. Ammonium nitrate or hydrogen were two potential ammonia derivatives that were identified as capable of enhancing aqueous ammonia ignition whilst reducing the required CR to 24. Şahin et al. [66] reported that as compared to a neat diesel engine, the fuel efficiency of diesel/aqueous NH_3 engine reduced by ~20% when the aqueous NH_3 volume fraction increased by 10%. HC and CO generally show decreasing trends as the NH_3 fraction increased. NO_x increased as NH_3 proportion increased.

Oxygenated fuels were another option that can conceivably enhance NH_3 combustion due to additional oxygen supply. Sivasubramanian et al. [67] showed that a 80/20 biodiesel/NH_3 engine reduced HC, CO, and smoke emissions by nearly 25% at full load. NO_x emissions from the biodiesel (BD)/NH_3 engine were about 300 pm higher than diesel but ~100 ppm lower than the biodiesel engine. Ryu et al. [68,69] showed that the exhaust emission from the ammonia/DME (Dimethyl Ether) engine did not enhance noticeably after improving fuel injection methods, denoting that post-exhaust treatment is still needed for the ammonia/DME engine operation. Lin & Lin [70] found that fuel efficiency for the biodiesel/NH_3 blend was

403 lower than neat biodiesel and diesel. CO and NO_x emissions for biodiesel/NH_3 blend were
404 lower than diesel by as much as 100 ppm for <1800 RPM engine speed. Gross & Kong [71]
405 showed that an increase in NH_3 volume fraction to 40% in the NH_3/DME blend elevated the
406 engine HRR by ~5 J/°CA against that of neat DME engines (2548 RPM). NO emissions for
407 neat DME and 40/60 NH_3/DME engines were found to be very similar. When pilot injection
408 was used, cylinder pressure and HRR increased by 20 bar and 20 J/°CA, respectively as the
409 mass flow for pilot injection increased to 50%. NO_x and CO emissions were not sensitive to
410 double injection. Unburned NH_3, however, reduced by ~30% as pilot injection increased to
411 50%. Bro & Pedersen [72] showed that the BTE of an NH_3 engine is higher than diesel at a
412 lower excess air ratio. Ignition delay for ammonia is higher than for methanol, ethanol, methane,
413 and diesel. Cylinder pressure for diesel and methane are higher than for NH_3. Excess air ratio
414 > 1.5 is needed to diminish CO emissions. NO_x emissions for NH_3 are higher than for other
415 fuels.

416 Ammonia decomposition, which was considerably successful in the SI engines, was
417 also tried out in CI engines. Wang et al. [73] utilised catalytic NH_3 decomposition in the CI
418 engine for that purpose. It was shown that the BTE of the diesel/H_2/NH_3 engine was very
419 similar to that of an Ultra-Low Sulphur Diesel (ULSD) engine, regardless of the variation in
420 H_2/NH_3 volume fraction. HC and CO decrease by ~7.5% when H_2/NH_3 volume fraction
421 increased from 2.47 to 11.03. NO emissions of the H_2/NH_3 engine were comparable with the
422 ULSD engine despite NO_2 being found marginally higher than that of the ULSD engine. Gill
423 et al. [74] examined combustion of gaseous neat NH_3, H_2, and dissociated NH_3 in a CI engine.
424 BSFC for a 75/1/24 H_2/NH_3/N_2 blend was found lower than for neat NH_3, indicating a better
425 fuel efficiency of the former. It was hypothesised that emissions from ammonia may be
426 enhanced through preheating the chemical (e.g. waste heat from the exhaust gas can be used to
427 partly decompose ammonia). Pochet et al. [75] noticed an increased resistance against

autoignition at around 15% vol. of ammonia in ammonia/hydrogen mixtures. The higher the ammonia loading is, the slower and lower the pressure and temperature will rise. Ammonia can create a two-fold reduction in maximum pressure rise rates (MPRR), with a combustion duration increasing from 3 to 7 °CA. Lamas & Rodriguez [56] examined the effects of ammonia injection in diesel/hydrogen engines. It was reported that optimum NO_x reduction (~60%) was obtained at 43.2 °CA aTDC. NO_x reduced drastically with increasing ammonia fraction. With increasing $NH_3/NO_i > 3$, un-reacted NH_3 becomes significant.

Lasocki et al. [76] showed that the Brake Specific Fuel Consumption (BSFC) of a diesel/NH_3 engine was ~25 g/kW-hr higher than that of a diesel engine. CO for the dual-fuel engine was noticeably lower than neat diesel while NO emissions were comparable for both engines. Hogerwaard & Dincer [77] showed that the efficiency and exergy destruction rate for the H_2 assisted NH_3/diesel engine was only slightly higher than for the neat diesel engine. NO_x emissions from the NH_3/diesel engine started to meet tier 2 and 3 requirements when NH_3 mass fraction exceeded 0.5. Reiter & Kong [78–80] examined diesel/NH_3 combustion in a CI engine. It was found that for a full load 1400 RPM turbocharged engine, 50% ammonia input power fraction could elevate the engine brake torque by 20 ft-lb as compared to a neat diesel engine, concurring with the findings by Pearsall & Garabedian [81] where BTE of the NH_3/diesel engine was found to be higher than neat diesel by approximately 10%. Furthermore, NO_x emissions from the diesel/NH_3 engine were 10 g/kW-hr lower than in the diesel engine, owing to the lower diesel/ammonia combustion temperature [78–80]. Disparities in UHC emissions from both engines were only marginal. Overall, diesel/ammonia combustion resulted in lower NO_x emissions than those produced by diesel for ammonia input power fraction < 60% [78–80]. Niki et al. [57–59] reported that peak cylinder pressure of a 1362 RPM 6 kW diesel/NH_3 engine was lowered marginally (~0.2 MPa) as the energy fraction of ammonia/diesel blend increased from 0 to 15%. N_2O, unburned NH_3, and CO emissions increased by 75 ppm, 3000

453 ppm, 25 ppm, respectively, denoting a drastic decline in combustion efficiency due to the
454 presence of NH_3.

455 By referring to Fig. 6, retarded fuel injection timing to aTDC is not exactly an ideal
456 approach for improving NH_3 combustion in CI engines. Although this approach reduced NO
457 emissions remarkably, it also resulted in a drastic increase of unburned NH_3. Aqueous ammonia
458 appears to be an ideal way of improving both performances and emissions. However, it should
459 be underlined that this method will most likely increase the noise level of the engine due to the
460 increased heat release in the pre-mixing burning stage. Blending the NH_3 with fossil diesel
461 commonly leads to enhanced engine HRR and higher NO emissions. Overall, the combustion
462 and emissions performances of neat NH_3 can be improved by optimising the mass flow and
463 timing for pilot and main injection, leading to simultaneous reduction of N_2-based emission
464 and increased engine HRR.
465

4.0 Ammonia in Gas Turbine

Constant volume combustion is undoubtedly desirable for ammonia combustion, mainly because it does not interrupt flame propagation like that in the reciprocating piston engine. Moreover, various combustion strategies/combustor modifications are easier for implementation when compared with reciprocating piston engines, owing to the absence of induction and exhaust systems at the top of the combustion chamber. Ammonia performances in jet engines has been investigated by several groups of researchers. Karabeyoglu et al. [82] found that blending the ammonia with JP4 with a mass fraction higher than 0.7 could reduce the carbon emission by at least 60%. Nonetheless, primary challenges in using ammonia arise from retarded ammonia kinetics that led to a lower flame temperature that augments flame instability. Iki et al. [83] examined ammonia combustion in a 50kW gas turbine. At 75,000 RPM gas turbine speed, NO emissions of NH_3/kerosene blends were increased by 1500 ppm as kerosene concentration decreased by 30%. The drastic increase in NO emissions poses a great challenge for ammonia-fuelled gas turbines, especially when it comes to aerospace applications [11,29,83,84].

Therefore, due to the NH_3 energy density, which is considerably lower than jet-fuel requirements [85], this review focuses only on land-based ammonia gas turbines. A premixed ammonia/air swirl combustor was examined by Hayakawa et al. [86]. It was reported that the cylindrical liner extended the lean blow-off (LBO) limit of the flame from φ = 0.8 to 0.6 for mixture inlet velocities up to 8 m/s. Increased swirl number led to narrowed stable flame regions, owing to the decrease in characteristic length scale [87]. The characteristic length scale of the recirculating flow was found independent of the swirl number for a low inlet velocity of 3.14 m/s. As inlet velocity increased to ~45 m/s, the stable flame regime was confined to $1.0 < \varphi < 1.2$ [9]. NO emissions were about 5000 ppm in the fuel-lean combustion but reduced to <10 ppm when $\varphi > 1.1$. Unburned NH_3 concentration showed reverse trends to NO where it

was nearly ~0 ppm in the fuel-lean regime but went up to > 5000 ppm at $\varphi \approx 1.1$. Emissions of both species were minimum at $\varphi \approx 1.05$, as shown in Fig. 7. The authors suggested that $\varphi \approx 1.05$ should be adopted for pure ammonia gas turbine operation [86]. Somarathne et al. [88] also observed a similar emissions trend through the numerical study of a bluff-body stabilised non-premixed NH_3/air swirl flame. NO emissions decreased by nearly 6000 ppm as global φ increased from stoichiometric to 1.4. Unburned NH_3 and H_2 were nearly zero in the fuel-lean regime but increased considerably (> 5000 ppm) when φ > 1.1 of which NH_3 increased by > 5000 ppm [86].

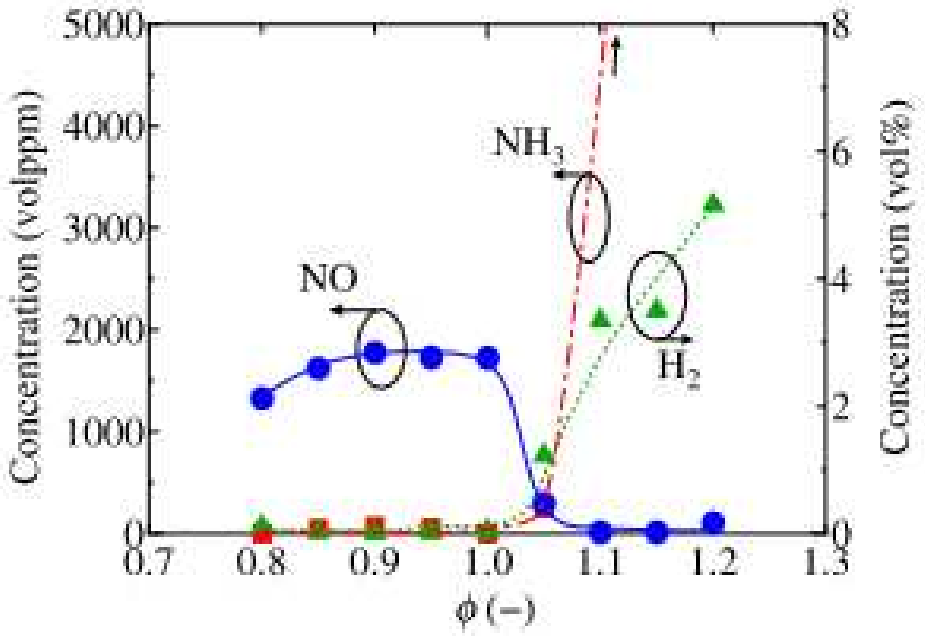

Fig. 7 NO, NH_3, and H_2 emissions for a cylindrical liner with 200 mm liner length with geometric swirl number (S_G) = 0.736 (reprint from [86] with permission from Elsevier)

Non-premixed NH_3/air combustion was one of the methods capable of improving the NO emission of NH_3/air combustion (Fig. 8) [88]. It was reported that NO emissions from these non-premixed stoichiometric NH_3/air combustion conditions was lower by a factor of 1.05 as compared to the premixed mode. However, at φ > 1, premixed combustion was constantly cleaner than non-premixed combustion in terms of lower NO emission [88]. Lower NO

emissions in non-premixed stoichiometric NH_3/air combustion was mainly due to the local heterogeneous φ and fuel-rich pockets formed in the central region of the combustor. These prohibit the formation of NO via thermal route as a result. Despite NO emissions from stoichiometric non-premixed NH_3/air combustion were lower than the premixed mode, the overall emissions remained exceptionally high (~5852 ppm). Furthermore, the concentration of unburned NH_3 was not examined. It would be expected that unburned NH_3 would be high in the non-premixed mode due to the heterogeneous φ. The performance of non-premixed NH_3/air combustion in an actual micro gas turbine (MGT) was examined by Osamu et al. [89]. It was demonstrated that MGT could operate from 70,000 RPM to 80,000 RPM with output power ranging from 18.4 kW to 44.4 kW. It was also hypothesised that a heterogeneous mixture would lead to higher unburned NH_3 emission than the premixed mode.

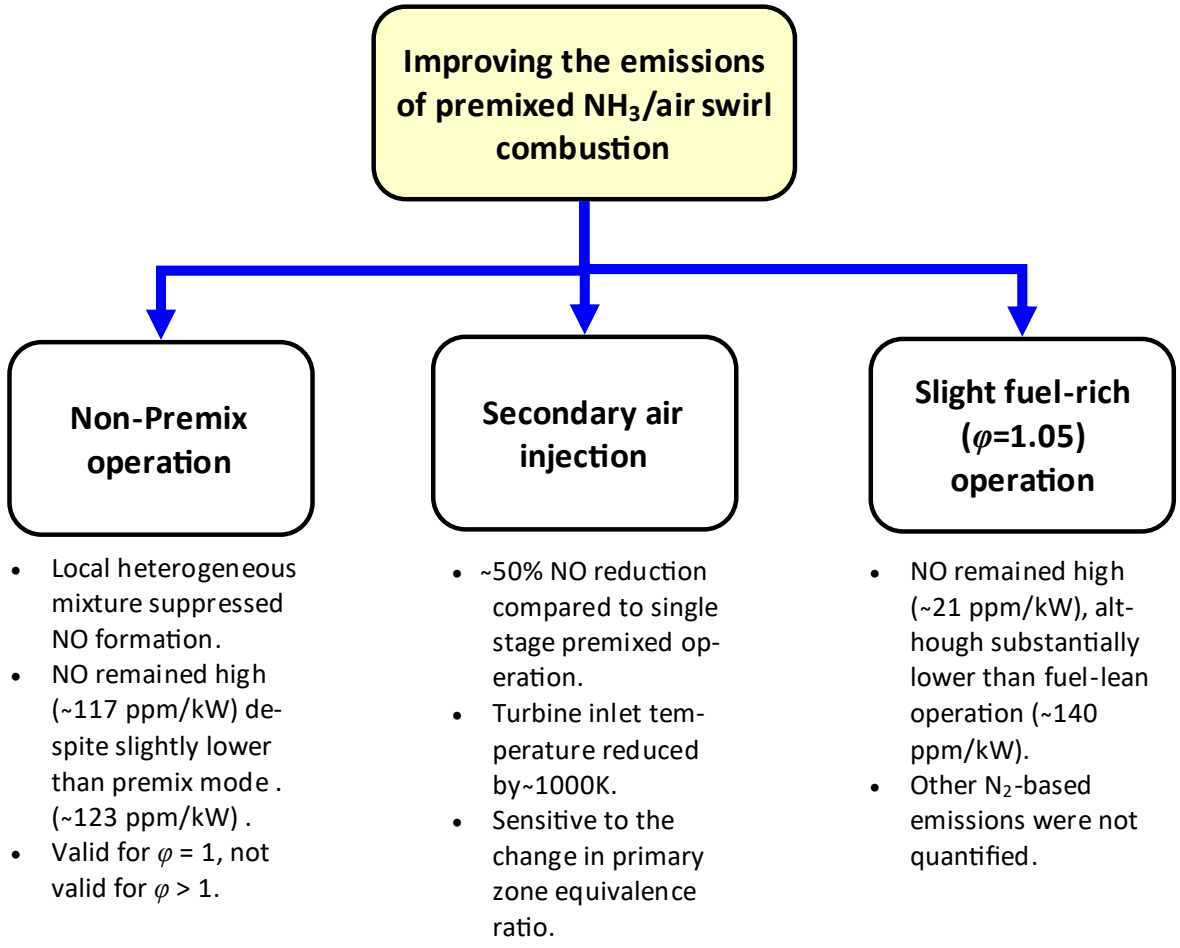

Fig. 8 Methods for improving the emissions performances of premixed pure NH_3/air swirl combustion. Results for AIST unit (Japan).

Okafor et al. [90] showed that non-premixed NH_3/air combustion is a cleaner solution over the premixed mode in a specific φ_{global} only. For $0.85 < \varphi_{global} < 1.1$ operation, NO emissions from premixed NH_3/air combustion were lower than the non-premixed operation by ~1200 ppmv. As φ_{global} dropped below 0.8, however, premixed combustion produced lower NO than the non-premixed operation. A slightly fuel-rich global φ (1.05) was again identified as an ideal operating point for both premixed and non-premixed NH_3/air combustion, where NO, NO_2, N_2O, and unburned NH_3 emissions were minimal [90]. These findings concur with Hayakawa et al. [86] and Somarathne et al. [88].

The idea of operating pure NH_3 combustion (premixed and non-premixed) at $\varphi \sim 1.05$ (Fig. 8) was attractive, mainly because NO and unburned NH_3 emission were the lowest at this specific φ (Fig. 7) [86]. However, it should be highlighted that NO emission from NH_3 combustion remained relatively high when compared with biodiesel and diesel (NH_3: 21 ppm/kW [86], biodiesel and diesel (~ 7.61 ppm/kW) [91,92]). Furthermore, other N_2-based emissions are expected to be higher owing to the reduction in airflow. The NH_x^* combination ($NH_x^* + NH_x^*$) was identified as one of the predominant reactions in fuel-rich NH_3 combustion [93]. NH_x^* combination produces NNH^* that is later consumed by O^* via $NNH + O \rightarrow NH + NO$ [94], denoting a vast majority of the NNH^* would lead to the production of NH^* in fuel-rich operation [95–97]. Furthermore, NH_x^* combination promotes the production of N_2H_x and HNO at high temperatures [98], preluding the production of NOx emissions. It was shown that the introduction of the N_2H_x reactions led to a more accurate estimation of NH^* and NH_2^* concentrations [99], signifying that N_2H_x are important elements in the fuel-rich NH_3 combustion.

In another attempt to improve NH_3 emissions performance, secondary air was injected into the post-reaction zone of the combustor. The NO emission from the global fuel-lean

548 NH_3/air premixed combustion was reduced by ~50% as compared to the single-stage
549 combustion when secondary air was introduced at near stoichiometric primary φ [100,101]. As
550 primary φ increased to 1.2, however, NO emission from the two-stages combustion turned out
551 to be higher than single-stage rich combustion, signifying that secondary air injection strategy
552 is highly sensitive to the change in primary φ. However, the unburned ammonia emissions
553 would be much higher without secondary combustion, thus making this strategy the preferred
554 by those working on ammonia gas turbine technologies. The 2 stages combustion was also
555 applied to non-premixed NH_3/air combustion. Okafor et al. [90] reported that a fuel stream
556 injection angle of 45° reduced NO emission by nearly 100 ppmv as compared to an injection
557 angle of 0° at global $\varphi = 0.3$. By increasing the area of the secondary dilution holes, Osamu et
558 al. [102] showed that NO_x could be reduced by nearly 2/3. Moreover, unburned NH_3 was also
559 reduced considerably. The authors claimed that the new combustor offered a promising cleaner
560 solution to non-premixed NH_3 gas turbine power generation. Despite secondary air injection
561 was effective in suppressing NO_x emission, but the combustor exit temperature was reduced
562 by ~1000 K due to secondary air injection [101]. Substantial reduction in combustor outlet
563 temperature (turbine inlet temperature) is expected to lower the thermal efficiency of the
564 turbine [103]. Moreover, NO_x emission at the combustor exit was sensitive to the changes in
565 the primary zone equivalence ratio (φ_{pri}). NO_x emissions at the combustor exit were reduced
566 by 79 ppm as compared to a combustor central injection when $\varphi_{pri} = 1.2$; but when $\varphi_{pri} = 1.25$,
567 NO_x emission at combustor exit were 220 ppm higher than with the central injection [90].
568 In addition to the conventional swirl burner, NH_3 combustion in Dry-Low Emissions
569 (DLE), Rich-burn, Quick-quench and Lean-burn (RQL), and Moderate or Intense Low Oxygen
570 Dilution (MILD) combustor have been also examined numerically [104]. It was shown that
571 DLE combustion is not ideal for NH_3 combustion, owing to the low NH_3 reactivity. RQL and
572 MILD combustor were found effective in suppressing the thermal NO_x formation. RQL

573 NH_3/H_2 combustion [105,106] also yielded promising emission reduction. By using H_2 pilot
574 injection at elevated inlet pressure and temperature, unburned NH_3 was reduced by a factor of
575 2 at stoichiometric combustion [105,106]. Nonetheless, authors [104] concluded that a high
576 level of dilution might pose challenges to the gas turbine operation. Similar to previous
577 combustion systems, a potential drawback of these combustors would be lower output
578 temperatures that reduce the heat quality delivered to the gas turbine (Fig. 8), although
579 simulations provided good temperatures within the range of those profiles produced by fossil
580 fuel blends.

581 CH_4 was proposed to assist neat ammonia combustion. Premixed NH_3/CH_4 combustion
582 was investigated by Valera-Medina et al. [107] using a generic swirl burner at different global
583 φ and CH_4 mass fractions. Flame instability was provoked when global $\varphi > 1.25$, owing to the
584 weakened central recirculation zone. The NO_x emission was remarkably low (< 20 ppm) when
585 $\varphi > 1.1$, mainly due to the consumption by NH_2^*. Elevated gas temperature in the post-flame
586 zone was attributed to the reaction $NH_2 + NO \rightarrow N_2H + OH$. Conversely, CO emission was
587 exceptionally high when $\varphi > 1.1$ (up to 900 ppm). In fuel-lean combustion, however, NO_x was
588 primarily produced via interactions between N^*, NH^* and O^*, as well as the reaction $HNO + H$
589 $\rightarrow NO + H_2$. Fig. *9* depicts emissions from NH_3/CH_4 combustion. As compared to premixed
590 fuel-lean NH_3/air combustion with NO_x emission of approximately 151.5 ppm/kW [86],
591 blending NH_3 with CH_4 lowered NO_x emission in the fuel-lean regime to about 69 ppm/kW
592 [107]. However, emissions performance of NH_3/CH_4 remain comparatively high when
593 compared to those of biodiesel, diesel, and natural gas [91,92]. Recently, Khateeb et al. [87]
594 observed that ammonia fraction in the fuel blend needs to be decreased to maintain flame
595 stability as mixture inlet velocity and thermal power increased.

596 Xiao et al. [108] showed that the presence of NH_3 in the NH_3/CH_4 fuel blends resulted
597 in prolonged mixture ignition delay as compared to neat methane. Ignition delay was increased

598 by a factor of 7.7 under the stoichiometric conditions as NH_3 mole fraction increased from 0%
599 to 80%, leading to flame speed reduction of ~200 mm/s. NO_x emissions were found to be
600 independent of NH_3 mole fraction in the fuel-rich regime (φ > 1.1). In the fuel-lean regime,
601 however, increased NH_3 mole fraction led to substantially high NO production. The NO
602 emission was elevated by approximately 50% as NH_3 mole fraction increased from 20% to
603 80% at φ = 0.8. CO emissions, however, increased drastically in fuel-rich combustion.
604 Nonetheless, increased NH_3 mole fraction from 20% to 80% lowered CO emission by a factor
605 of 4 at φ = 1.6. A strong correlation between NO and CO emissions and HNO and HCO radical
606 concentrations was identified [108].
607 In another study by Xiao et al. [109], Tian's and Teresa's mechanisms for NH_3/CH_4
608 combustion were enhanced. NH + OH → HNO + H reaction was found to be the most dominant
609 reaction for NO formation in fuel-lean operation while reactions NH_2 + NO → NNH + OH and
610 N +NO → N_2 + O play important roles for the NO consumption under elevated conditions.
611 Meanwhile, reactions $CH_3 + O_2 \rightarrow CH_2O + OH$ and NH_3 +OH → $NH_2 + H_2O$ have the largest
612 impact on OH radical production under elevated conditions. The reaction NH + OH → HNO
613 + H (+M) plays the key role in the NO formation process, the conversion from HNO to NO is
614 mainly through HNO + M → H + M (45.4% contribution). HNO + H → NO + H_2 and HNO +
615 OH → NO + H_2 are also active but with a smaller net contribution to the NO formation [109].
616

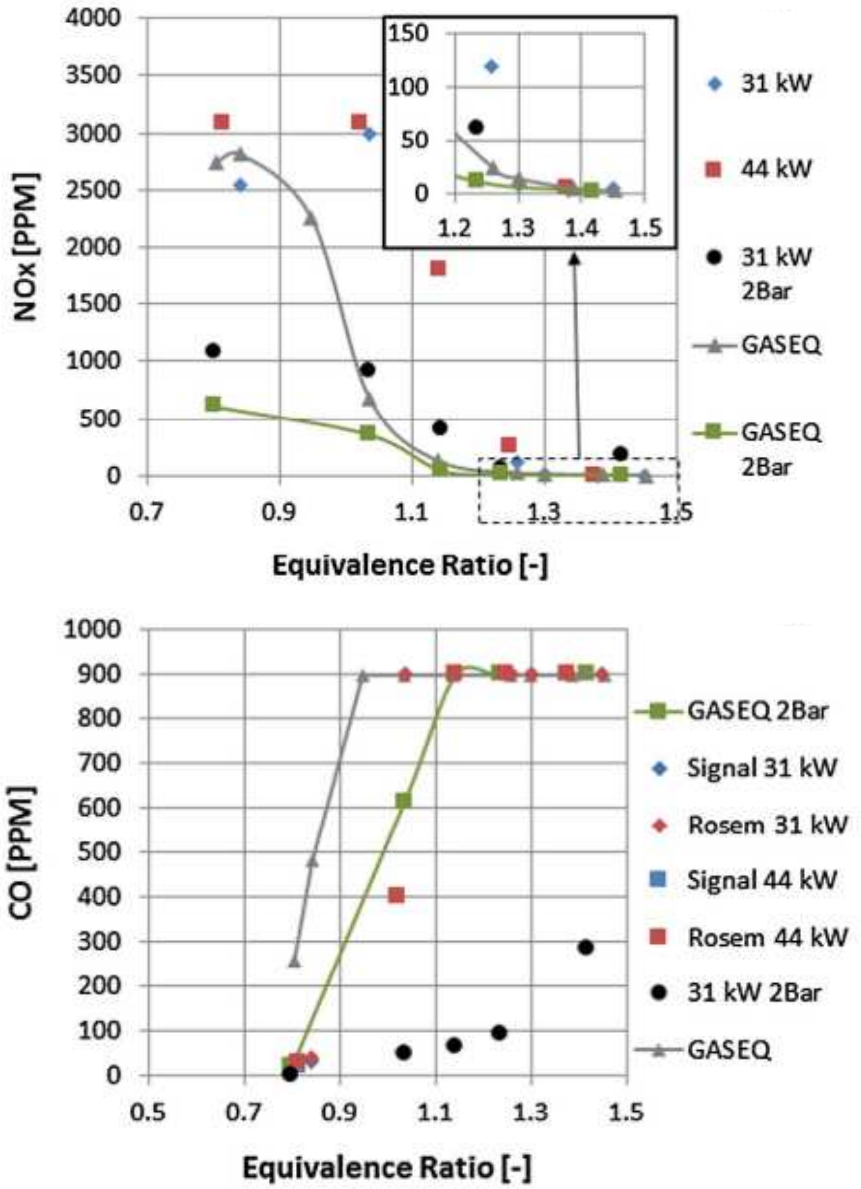

Fig. 9 NO_x emission (top) and CO emission (bottom) from NH_3/CH_4 combustion in model gas turbine combustor (reprint from [107])

Somarathne et al. [110] examined non-premixed CH_4/NH_3/air swirl combustion under elevated conditions. NO emissions for the fuel-lean CH_4/NH_3/air combustion increased by nearly three orders of magnitude when NH_3 energy fraction increased from 0% to 40%. A recent study by Okafor et al. [90,111] concluded that fuel-lean non-premixed NH_3/CH_4 combustion resulted in a more promising NO reduction as compared to fuel-lean premixed NH_3/CH_4 combustion. It was shown that premixed NH_3/CH_4/air combustion increased NO

627 emission by a factor of 1.26 when compared with premixed NH_3/air combustion. Conversely,
628 non-premixed NH_3/CH_4 combustion reduced NO emission by a factor of 2.2 as compared to
629 non-premixed NH_3 combustion [90,111]. Moreover, NO_2 and N_2O emissions from premixed
630 NH_3/CH_4 combustion were also found to be considerably higher than non-premixed NH_3/CH_4.
631 The authors concluded that fuel-bound nitrogen is the predominant NO formation mechanism
632 in NH_3/CH_4 combustion. However, it should be underlined that the premixed combustion used
633 in [90,111] was different from typical practice [107]. As shown in Fig. 10a, the flow of
634 premixed combustible mixture (reactants + air) was divided between swirler and fuel injector
635 inlet [90,111]. A typical premixed burner, however, channels the premixed combustible
636 mixture from burner inlet to burner outlet without passing through the injector (Fig. 10b) [107].
637 The remarkably different premixing strategy may be contributing to the findings where non-
638 premixed combustion was cleaner than the fully premixed mode.
639

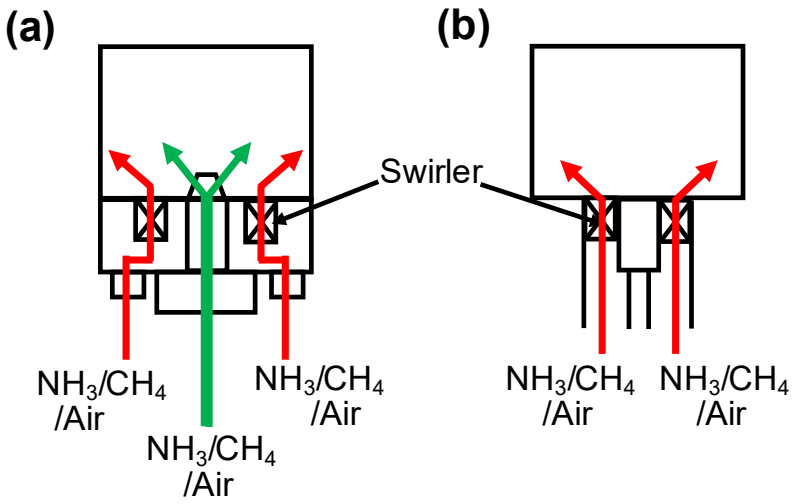

640
641 Fig. 10 (a) Partial premixed swirl combustor used by [111], (b) Typical premixed combustion
642 in swirl burner.
643
644

645 H_2 is undeniably an ideal blending agent for assisting NH_3 combustion as seen in
646 section 2. NH_3/H_2 combustion in a constant volume combustor was also investigated. Valera-
647 Medina et al. [112] reported that premixed NH_3/H_2 swirl combustion could establish a decent
648 flame for global φ as low as 0.41 using swirl number S_G = 1.05. At φ = 0.52, however, flame
649 instability was incited. Exceptionally high NO_x emissions (> 1000 ppm for φ > 0.5) from
650 NH_3/H_2 combustion were attributed to the excess OH^* and O^* production in the fuel-lean
651 combustion regime. By lowering S_G to 0.8 and hydrogen mass fraction to 30%, Valera-Medina
652 et al. [113] reported a monotonic reduction in OH^* intensities when φ increased from 1.0 to 1.3
653 despite lacking oxygen in the fuel-rich regime, denoting an only marginal change in the heat
654 release location and flame position. Steam injection was also attempted, showing an effective
655 method in reducing NO formation [114]. The NO_x emission was reduced by nearly an order of
656 magnitude while laminar flame speed reduced by nearly 10 cm/s as the steam flow rate
657 increased from 0 g/s to 0.6 g/s at φ = 1.2 [114]. The O^* was consumed via reaction $O + H_2O$
658 $\rightarrow 2OH$ to produce OH^*, thus reducing the NO formation by restricting the production of HNO.
659 Nonetheless, excessive OH^* produced at lower temperature reaction promotes the production
660 of NH_2^* at the post-reaction zone [115]. Guteša Božo et al. [116] also reported on positive
661 attributes of steam addition in NO reduction. It was reported that the use of steam mass fraction
662 up to 0.4 was possible, where the flame showed low fluctuation and good stability [116].

663 Like NH_3/air and NH_3/CH_4/air combustion, fuel-lean NH_3/H_2 swirl combustion also
664 suffers from exceptionally high NO_x emission. This is mainly attributed to the high O^*, OH^*,
665 and H^* that led to HNO (precursor of NO) formation. Likewise, there was also a proposal to
666 operate NH_3/H_2 combustion in the fuel-rich regime where NO consumption is prevalent [117].
667 Fortunately, NO reaction with NH_2^* can lead to the formation of N_2 and H_2O, especially at
668 fuel-rich operation. However, high temperature of reaction can lead into another direction, a
669 path that goes from NH2 to $NNH^* + OH^*$ instead of $N_2 + H_2O$. The OH^* intensity could be

found nearly constant when φ varies from 1-1.3, due to the NO consumption by NH_2^* [113]. A secondary pathway also leads to the reaction of NH_x^* with O^*, OH^*, or H^* leading to the formation of other NH_x radicals. However, well controlled conditions and temperature under fuel-rich conditions are expected to deliver low NOx with high N_2 and H_2O when using NH_3/H_2 combustion [113], inferring that fuel-rich operation is the best strategy to burn ammonia/hydrogen blends.

Partial premixed NH_3/H_2 swirl combustion was recently examined by researchers from Cardiff University. In contrast to the conventional premixed combustion where reactants and oxidiser were premixed prior to entering the combustor, Fig. 11(a), the NH_3 was channelled to the combustor outlet via central injection lance in partially premixed combustion as shown in Fig. 11(b). Remarkably low NO_x emission was achieved at the expense of high NH^* and NH_2^* production [118]. Combustion efficiency is expected to be lower to fully premixed due to a greater portion of unburned NH_3. High NH^* and NH_2^* concentrations in the partial premixed NH_3/H_2 combustion is due to the local fuel-rich condition that arises from the inferior central fuel jet penetration into the reacting shear layer formed by a swirling premixed H_2/air flow. A pressurised central fuel jet is likely to scatter NH_3 more uniformly across the reacting shear layer. Highly reactive OH^*, H^*, and O^* produced by swirling premixed H_2/air reactions are mainly clustered in the shear layer. These radicals would subsequently promote NH_3 consumption, leading to a more complete NH_3/H_2 combustion.

Another partially premixed concept was proposed and examined by Franco et al. [119]. The fuel mixture (NH_3/H_2) was mixed tangentially with axial airflows at the verge of a swirler inlet as depicted in Fig. 11(c). The lean blowoff limit for the NH_3/H_2 swirl flame was stretched to $\varphi = 0.3$ for NH_3 mole fraction 0.7. However, the study was performed using an input thermal power of only 1.9 kW. Substantially low mixture inlet velocity renders a sufficient time scale for ammonia to react with hydrogen, comprising a possible reason for the extended flame

operating regime observed. The level of O_2 in the flue gas increased by about 2% as the NH_3 mole fraction increased from 0.7 to 0.9, signifying poorer NH_3 oxidation when its mole fraction > 0.7.

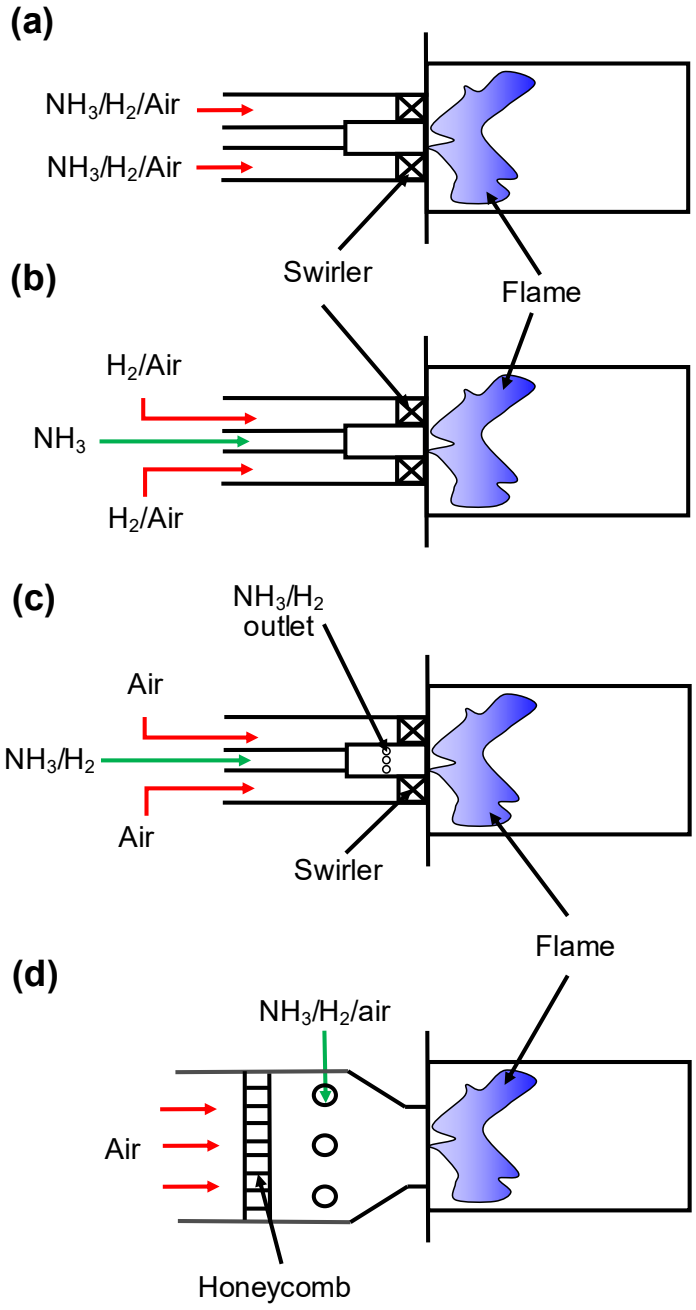

Fig. 11 Schematic diagram for (a) Typical premixed NH_3/H_2/air combustion, (b) Partial premixed NH_3/H_2/air combustion by [118], (c) Partial premixed NH_3/H_2/air combustion by [119], (d) Partial premixed NH_3/H_2/air combustion by [120].

Fig. 11(d) shows a partially premixed concept introduced by Zhu et al. [120]. A fraction of air was blended with NH_3/H_2 and then mixed with the remaining tangential airflow prior to the reach the combustor outlet. The flame blow-off limit of NH_3/H_2 partial premixed combustion was extended to $\varphi \sim 0.4$. Their design successfully reduced NO emission to < 100 ppm. Moreover, NH_3 fuel fraction could be increased to as high as 80%. The NO reduction was notably when compared with 1000 ppm at $\varphi \sim 0.65$ using the same NH_3 fuel fraction. The significant reduction in NO emission was attributed to the drastic decrease in OH^*. Partially premixed NH_3/H_2 combustion has received considerable attention lately to improve NH_3/H_2 emission performances. The concept by Pugh et al. [118] was based on forming local fuel-rich pockets in the middle of the reaction zone. The design proposed by Zhu et al. [120] and Franco et al. [119], however, were based on extending the LBO limit to a leaner regime to lower the post-combustion emissions. Such an approach was possible due the partially premixed operation incorporates non-premixed combustion that is less vulnerable to the turbulence fluctuations in the fuel-lean operation. However, the results proposed by Zhu et al. did not deliver details of unburned ammonia and other NOx species (i.e. N2O and NO2), thus requiring further analyses to demonstrate the applicability of burning under fuel-lean conditions ammonia/hydrogen blends. These works are currently taking place, with further data to be published in the following months.

5.0 Conclusions

The development of ammonia combustion technologies in SI engine, CI engine, and GT have been reviewed. H_2 is the most used additive to assist NH_3 combustion in the SI engine. H_2 was inducted into SI engine either through NH_3 cracking or a separate H_2 supply. The NH_3 cracking system resulted in more superior engine performance than the separate H_2 supply system. This is presumably due to the higher H_2/NH_3 mass ratio in the NH_3 cracking system. Increased H_2 mass fraction >10% in the separate H_2 supply system is expected to allow comparable engine performances with that of the NH_3 cracking system. Engine parameters optimisation may be needed for H_2 mass fraction >10% due to the increase in turbulent flame speed.

As for CI engines, there has been a recurrent idea of retarding the ammonia injection timing. This approach undesirably elevates unburned NH_3 emission despite leading to substantial NO reduction. Aqueous ammonia could improve engine HRR and emissions performances, but it also increases the noise level of the engine undesirably due to the steep heat release increase rate in the pre-mixing burning stage. Mass flow and timing optimisation for multiple injection techniques is seemingly a more promising approach to reduce N_2-based emissions and enhance CI engine HRR concurrently.

NH_3 combustion strategies in the GT can be mainly divided into two approaches, extending the LBO limit to φ<0.4, and fuel-rich (φ~1.05-1.25) operation. Partially premixed combustion that incorporates the advantages of both premixed and non-premixed combustion have attracted considerable attention lately, due to its capability to reach φ~0.4 while retaining reasonable flame stability and low NO emissions. This review shows that combustion and emissions performances of NH_3 can be improved by innovation in combustion technologies. This, combined with the advancement of advanced and cost-effective ammonia production

748 technologies based on renewable resources, will make ammonia an important component of
749 the future energy mix.

References

[1] Reddy PJ. Clean Coal Technologies for Power Generation. CRC Press; 2014.

[2] International Energy Agency. Electricity Information 2019. 2019.

[3] The National Aeronautics and Space Administration. Global Climate Change - Vital Signs of the Planet 2020. https://climate.nasa.gov/vital-signs.

[4] The Royal Society. Ammonia : fuel and energy store 2020.

[5] Valera-Medina A, Amer-Hatem F, Azad AK, Dedoussi IC, Joannon M de, Fernandes RX, et al. A review on ammonia as a potential fuel : from synthesis to economics. Energy & Fuels 2021:1–108.

[6] Valera-Medina A, Xiao H, Owen-Jones M, David WIF, Bowen PJ. Ammonia for power. Prog Energy Combust Sci 2018;69:63–102.

[7] Newhall HK, Starkman ES. Theoretical Performance of Ammonia as a Gas Turbine Fuel. SAE Trans 1967;75:772–84.

[8] Verkamp FJ, Hardin MC, Williams JR. Ammonia combustion properties and performance in gas-turbine burners. Symp Combust 1967;11:985–92.

[9] Kobayashi H, Hayakawa A, Somarathne KDKA, Okafor EC. Science and technology of ammonia combustion. Proc Combust Inst 2019;37:109–33.

[10] Law CK. Combustion Physics. Cambridge University Press; 2006.

[11] Li J, Huang H, Kobayashi N, He Z, Nagai Y. Study on using hydrogen and ammonia as fuels: Combustion characteristics and NOx formation. Int

772 J Energy Res 2014;38:1214–23.
773 [12] Mathieu O, Petersen EL. Experimental and modeling study on the high-
774 temperature oxidation of Ammonia and related NOx chemistry. Combust
775 Flame 2015;162:554–70.
776 [13] Breeze P. An Introduction to Piston Engine Power Plants. Pist. Engine-
777 Based Power Plants, 2018.
778 [14] U.S. Energy Information Administration (EIA). Natural gas-fired
779 reciprocating engines are being deployed more to balance renewables
780 2019. https://www.eia.gov/todayinenergy/detail.php?id=37972.
781 [15] Breeze P. Power Generation Technologies. 3rd ed. Elsevier; 2019.
782 [16] Mom AJA. Introduction to gas turbine. In: Jansohn P, editor. Mod. gas
783 turbine Syst., Woodhead Publishing; 2013.
784 [17] U.S. Energy Information Administration (EIA). Preliminary Monthly
785 Electric Generator Inventory (based on Form EIA-860M as a supplement
786 to Form EIA-860) 2021. https://www.eia.gov/electricity/data/eia860m/.
787 [18] Cornelius W, Huellmantel LW, Mitchell HR. Ammonia as an engine fuel.
788 SAE Tech Pap 1965:650052.
789 [19] Grannell SM, Assanis DN, Bohac S V., Gillespie DE. The operating
790 features of a stoichiometric, ammonia and gasoline dual fueled spark
791 ignition engine. Int. Mech. Eng. Congr. Expo., Chicago, Illinois, USA:
792 2006, p. 1–13.
793 [20] Grannell SM, Assanis DN, Bohac S V., Gillespie DE. The fuel mix limits

794 and efficiency of a stoichiometric, ammonia, and gasoline dual fueled
795 spark ignition engine. J Eng Gas Turbines Power 2008;130:042802.
796 [21] Grannell SM, Assanis DN, Gillespie DE, Bohac S V. Exhaust Emissions
797 from a Stoichiometric, Ammonia and Gasoline Dual Fueled Spark Ignition
798 Engine. Intern. Combust. Engine Div. 2009 Spring Tech. Conf.,
799 Milwaukee, Wisconsin, USA: 2009, p. ICES2009-76131.
800 [22] Lhuillier C, Brequigny P, Contino F, Rousselle C. Performance and
801 Emissions of an Ammonia-Fueled SI Engine with Hydrogen Enrichment.
802 SAE Tech Pap 2019:2019-24–0137.
803 [23] Lhuillier C, Brequigny P, Contino F, Rousselle C. Combustion
804 Characteristics of Ammonia in a Modern Spark-Ignition Engine. SAE
805 Tech Pap 2019:2019-24–0237.
806 [24] Lhuillier C, Brequigny P, Contino F, Mounaïm-Rousselle C. Experimental
807 study on ammonia/hydrogen/air combustion in spark ignition engine
808 conditions. Fuel 2020;269:117448.
809 [25] Sawyer RF, Starkman ES, Muzio L, Schmidt WL. Oxides of nitrogen in
810 the combustion products of an ammonia fueled reciprocating engine. SAE
811 Tech Pap 1968:680401.
812 [26] Starkman ES, James GE, Newhall HK. Ammonia as a diesel engine fuel:
813 Theory and application. SAE Tech Pap 1967:670946.
814 [27] Comotti M, Frigo S. Hydrogen generation system for ammonia-hydrogen
815 fuelled internal combustion engines. Int J Hydrogen Energy

816 2015;40:10673–86.
817 [28] Frigo S, Gentili R. Analysis of the behaviour of a 4-stroke Si engine
818 fuelled with ammonia and hydrogen. Int J Hydrogen Energy
819 2013;38:1607–15.
820 [29] Ryu K, Zacharakis-Jutz GE, Kong SC. Performance enhancement of
821 ammonia-fueled engine by using dissociation catalyst for hydrogen
822 generation. Int J Hydrogen Energy 2014;39:2390–8.
823 [30] Frigo S, Roberto Gentili, Angelis F De. Further Insight into the Possibility
824 to Fuel a SI Engine with Ammonia plus Hydrogen. SAE Tech Pap
825 2014:2014-32–0082.
826 [31] Ezzat MF, Dincer I. Development and assessment of a new hybrid vehicle
827 with ammonia and hydrogen. Appl Energy 2018;219:226–39.
828 [32] Ezzat MF, Dincer I. Comparative assessments of two integrated systems
829 with/without fuel cells utilizing liquefied ammonia as a fuel for vehicular
830 applications. Int J Hydrogen Energy 2018;43:4597–608.
831 [33] Frigo S, Gentili R, Doveri N. Ammonia plus hydrogen as fuel in a S.I.
832 engine: Experimental results. SAE Tech. Pap., vol. 4, 2012, p. 2012-32–
833 0019.
834 [34] Mørch CS, Bjerre A, Gøttrup MP, Sorenson SC, Schramm J.
835 Ammonia/hydrogen mixtures in an SI-engine: Engine performance and
836 analysis of a proposed fuel system. Fuel 2011;90:854–64.
837 [35] Westlye FR, Ivarsson A, Schramm J. Experimental investigation of

838 nitrogen based emissions from an ammonia fueled SI-engine. Fuel
839 2013;111:239–47.
840 [36] Ryu K, Zacharakis-Jutz GE, Kong SC. Effects of gaseous ammonia direct
841 injection on performance characteristics of a spark-ignition engine. Appl
842 Energy 2014;116:206–15.
843 [37] Zamfirescu C, Dincer I. Using ammonia as a sustainable fuel. J Power
844 Sources 2008;185:459–65.
845 [38] Zamfirescu C, Dincer I. Ammonia as a green fuel and hydrogen source for
846 vehicular applications. Fuel Process Technol 2009;90:729–37.
847 [39] Haputhanthri SO. Ammonia Gasoline Fuel Blends: Feasibility Study of
848 Commercially Available Emulsifiers and Effects on Stability and Engine
849 Performance. SAE Tech Pap 2014:2014-01–2759.
850 [40] Haputhanthri SO, Fleming J, Maxwell TT, Austin C. Ammonia and
851 gasoline fuel blends for internal combustion engines. 8th Int. Conf.
852 Energy Sustain., 2014, p. ES2014-6538.
853 [41] Haputhanthri SO, Maxwell TT, Fleming J, Austin C. Ammonia and
854 gasoline fuel blends for spark ignited internal combustion engines. J
855 Energy Resour Technol 2015;137:062201.
856 [42] Haputhanthri SO, Maxwell TT, Fleming J, Austin C. Ammonia Gasoline-
857 Ethanol/Methanol Tertiary Fuel Blends as an Alternate Automotive Fuel.
858 Proc. ASME 2014 Int. Mech. Eng. Congr. Expo., Montreal, Quebec,
859 Canada: 2014, p. IMECE2014-38026.

860 [43] Lhuillier C, Brequigny P, Contino F, Mounaïm-Rousselle C. Experimental
861 investigation on ammonia combustion behavior in a spark-ignition engine
862 by means of laminar and turbulent expanding flames. Proc Combust Inst
863 2020;000:1–10.
864 [44] Duynslaegher C, Jeanmart H, Vandooren J. Flame structure studies of
865 premixed ammonia/hydrogen/oxygen/argon flames: Experimental and
866 numerical investigation. Proc Combust Inst 2009;32 I:1277–84.
867 [45] United Nations Framework Convention on Climate Change. Global
868 Warming Potentials (IPCC Second Assessment Report) 2021.
869 https://unfccc.int/process/transparency-and-reporting/greenhouse-gas-
870 data/greenhouse-gas-data-unfccc/global-warming-potentials.
871 [46] Kass M, Abdullah Z, Biddy M, Drennan C, Hawkins T, Jones S, et al.
872 Understanding the Opportunities of Biofuels for Marine Shipping. 2018.
873 [47] Hsieh C-WC, Felby C. Biofuels for the marine shipping sector. 2017.
874 [48] International Maritime Organization. Sulphur 2020 – cutting sulphur
875 oxide emissions. Focus 2020.
876 http://www.imo.org/en/MediaCentre/HotTopics/Pages/Sulphur-2020.aspx.
877 [49] Niki Y, Nitta Y, Sekiguchi H, Hirata K. Diesel Fuel Multiple Injection
878 Effects on Emission Characteristics of Diesel Engine Mixed Ammonia
879 Gas Into Intake Air. J Eng Gas Turbines Power 2019;141.
880 [50] Reiter AJ, Kong S-C. Demonstration of Compression-Ignition Engine
881 Combustion Using Ammonia in Reducing Greenhouse Gas Emissions.

Energy & Fuels 2008;22:2963–71.

[51] Reiter AJ, Kong S-C. Combustion and emissions characteristics of compression-ignition engine using dual ammonia-diesel fuel. Fuel 2011;90:87–97.

[52] Gill SS, Chatha GS, Tsolakis A, Golunski SE, York APE. Assessing the effects of partially decarbonising a diesel engine by co-fuelling with dissociated ammonia. Int J Hydrogen Energy 2012;37:6074–83.

[53] Niki Y, Nitta Y, Sekiguchi H, Hirata K. Diesel Fuel Multiple Injection Effects on Emission Characteristics of Diesel Engine Mixed Ammonia Gas Into Intake Air. J Eng Gas Turbines Power 2019;141.

[54] Heywood JB. Internal Combustion Engine Fundamentals. 2nd ed. Mc-GrawHill; 2018.

[55] Lamas Galdo MI, Castro-Santos L, Vidal CGR. Numerical analysis of NOx reduction using ammonia injection and comparison with water injection. J Mar Sci Eng 2020;8.

[56] Lamas MI, Rodriguez CG. Numerical model to analyze NOx reduction by ammonia injection in diesel-hydrogen engines. Int J Hydrogen Energy 2017;42:26132–41.

[57] Niki Y, Nitta Y, Sekiguchi H, Hirata K. Diesel fuel multiple injection effects on emission characteristics of diesel engine mixed ammonia gas into intake air. J Eng Gas Turbines Power 2019;141.

[58] Niki Y, Nitta Y, Sekiguchi H, Hirata K. Emission and combustion

characteristics of diesel engine fumigated with ammonia. ASME 2018 Intern. Combust. Engine Div. Fall Tech. Conf. ICEF 2018, San Diego, CA, USA: 2018, p. ICEF2018-9634.

[59] Niki Y, Yoo DH, Hirata K, Sekiguchi H. Effects of ammonia gas mixed into intake air on combustion and emissions characteristics in diesel engine. Proc. ASME 2016 Intern. Combust. Engine Fall Tech. Conf., Greenville, SC, USA: 2016, p. ICEF2016-9364.

[60] Tay KL, Yang W, Chou SK, Zhou D, Li J, Yu W, et al. Effects of Injection Timing and Pilot Fuel on the Combustion of a Kerosene-diesel/Ammonia Dual Fuel Engine: A Numerical Study. Energy Procedia 2017;105:4621–6.

[61] Tay KL, Yang W, Li J, Zhou D, Yu W, Zhao F, et al. Numerical investigation on the combustion and emissions of a kerosene-diesel fueled compression ignition engine assisted by ammonia fumigation. Appl Energy 2017;204:1476–88.

[62] Lee D, Song HH. Development of combustion strategy for the internal combustion engine fueled by ammonia and its operating characteristics. J Mech Sci Technol 2018;32:1905–25.

[63] Lamas MI, Rodriguez CG. NOx reduction in diesel-hydrogen engines using different strategies of ammonia injection. Energies 2019;12.

[64] Pyrc M, Gruca M, Jamrozik A, Tutak W, Juknelevičius R. An experimental investigation of the performance, emission and combustion

stability of compression ignition engine powered by diesel and ammonia solution (NH4OH). Int J Engine Res 2020.

[65] Schönborn A. Aqueous solution of ammonia as marine fuel. Proc Inst Mech Eng Part M J Eng Marit Environ 2020.

[66] Şahin Z, Ziya Akcanca İ, Durgun O. Experimental investigation of the effects of ammonia solution (NH3OH) on engine performance and exhaust emissions of a small diesel engine. Fuel 2018;214:330–41.

[67] Sivasubramanian R, Sajin JB, Omanakuttan Pillai G. Effect of ammonia to reduce emission from biodiesel fuelled diesel engine. Int J Ambient Energy 2019.

[68] Ryu K, Zacharakis-Jutz GE, Kong SC. Performance characteristics of compression-ignition engine using high concentration of ammonia mixed with dimethyl ether. Appl Energy 2014;113:488–99.

[69] Ryu KH, Zacharakis-Jutz G, Kong SC. Effects of fuel compositions on diesel engine performance using ammonia-DME mixtures. SAE Tech Pap 2013;2:2013-01–1133.

[70] Lin CY, Lin HA. Engine performance and emission characteristics of a three-phase emulsion of biodiesel produced by peroxidation. Fuel Process Technol 2007;88:35–41.

[71] Gross CW, Kong SC. Performance characteristics of a compression-ignition engine using direct-injection ammonia-DME mixtures. Fuel 2013;103:1069–79.

948 [72] Bro K, Pedersen PS. Alternative diesel engine fuels: An experimental
949 investigation of methanol, ethanol, methane and ammonia in a D.I. diesel
950 engine with pilot injection. SAE Tech Pap 1977:770794.
951 [73] Wang W, Herreros JM, Tsolakis A, York APE. Ammonia as hydrogen
952 carrier for transportation; Investigation of the ammonia exhaust gas fuel
953 reforming. Int J Hydrogen Energy 2013;38:9907–17.
954 [74] Gill SS, Chatha GS, Tsolakis A, Golunski SE, York APE. Assessing the
955 effects of partially decarbonising a diesel engine by co-fuelling with
956 dissociated ammonia. Int J Hydrogen Energy 2012;37:6074–83.
957 [75] Pochet M, Jeanmart H, Contino F. A 22:1 Compression Ratio Ammonia-
958 Hydrogen HCCI Engine: Combustion, Load, and Emission Performances.
959 Front Mech Eng 2020;6:1–16.
960 [76] Lasocki J, Bednarski M, Sikora M. Simulation of ammonia combustion in
961 dual-fuel compression-ignition engine. 2nd Int. Conf. Sustain. Energy
962 Environ. Dev., vol. 214, 2019, p. 012081.
963 [77] Hogerwaard J, Dincer I. Comparative efficiency and environmental
964 impact assessments of a hydrogen assisted hybrid locomotive. Int J
965 Hydrogen Energy 2016;41:6894–904.
966 [78] Reiter AJ, Kong SC. Demonstration of compression-ignition engine
967 combustion using ammonia in reducing greenhouse gas emissions. Energy
968 and Fuels 2008;22:2963–71.
969 [79] Reiter AJ, Kong SC. Combustion and emissions characteristics of

compression-ignition engine using dual ammonia-diesel fuel. Fuel 2011;90:87–97.

[80] Reiter AJ, Kong S. Diesel Engine Operation Using Ammonia as a Carbon-Free Fuel. Intern. Combust. Engine Div. Fall Tech. Conf., San Antonio, Texas, USA: ASME; 2010, p. ICEF2010-35026.

[81] Pearsall TJ, Garabedian CG. Combustion of Anhydrous Ammonia in Diesel Engine. SAE Tech Pap 1967:670947.

[82] Karabeyoglu A, Evans B, Stevens J, Cantwell B. Development of ammonia based fuels for environmentally friendly power generation. 10th Annu. Int. Energy Convers. Eng. Conf. IECEC 2012, Atlanta, Georgia: AIAA; 2012, p. 1–27.

[83] Iki N, Kurata O, Matsunuma T, Inoue T, Suzuki M, Tsujimura T, et al. Micro gas turbine firing kerosene and ammonia. Proc. ASME Turbo Expo 2015 Turbine Tech. Conf. Expo., Montréal, Canada: 2015, p. GT2015-43689.

[84] Kurata O, Iki N, Matsunuma T, Inoue T, Suzuki M, Tsujimura T, et al. ICOPE-15-1139 Power generation by a micro gas turbine firing kerosene and ammonia. Proc Int Conf Power Eng 2015;2015.12:_ICOPE-15--_ICOPE-15-.

[85] Blakey S, Rye L, Wilson CW. Aviation gas turbine alternative fuels: A review. Proc Combust Inst 2011;33:2863–85.

[86] Hayakawa A, Arakawa Y, Mimoto R, Somarathne KDKA, Kudo T,

992 Kobayashi H. Experimental investigation of stabilization and emission
993 characteristics of ammonia/air premixed flames in a swirl combustor. Int J
994 Hydrogen Energy 2017;42:14010–8.
995 [87] Khateeb AA, Guiberti TF, Zhu X, Younes M, Jamal A, Roberts WL.
996 Stability limits and exhaust NO performances of ammonia-methane-air
997 swirl flames. Exp Therm Fluid Sci 2020;114:110058.
998 [88] Somarathne KDKA, Colson S, Hayakawa A, Kobayashi H. Modelling of
999 ammonia / air non-premixed turbulent swirling flames in a gas turbine-like
1000 combustor at various pressures. Combust Theory Model 2018;22:973–97.
1001 [89] Kurata O, Iki N, Matsunuma T. Performances and emission characteristics
1002 of NH3-air and NH3-CH4-air combustion gas-turbine power generations.
1003 Proc Combust Inst 2017;36:3351–9.
1004 [90] Okafor EC, Somarathne KDKA, Hayakawa A, Kudo T, Kurata O, Iki N.
1005 Towards the development of an efficient low-NOx ammonia combustor
1006 for a micro gas turbine. Proc Combust Inst 2019;37:4597–606.
1007 [91] Chiong M-C, Valera-Medina A, Chong WWF, Chong CT, Mong GR,
1008 Mohd Jaafar MN. Effects of swirler vane angle on palm biodiesel/natural
1009 gas combustion in swirl-stabilised gas turbine combustor. Fuel
1010 2020;277:118213.
1011 [92] Chong CT, Chiong M-C, Ng J-H, Lim M, Tran M-V, Valera-Medina A, et
1012 al. Oxygenated sunflower biodiesel: Spectroscopic and emissions
1013 quantification under reacting swirl spray conditions. Energy

2019;178:804–13.

[93] Haynes BS. Reactions of Ammonia and Nitric Oxide in the Burnt Gases of Fuel-Rich Hydrocarbon-Air Flames. Combust Flame 1977;28:81–91.

[94] Dean AM, Chou M, Stern D. Kinetics of rich ammonia flames. Int J Chem Kinet 1984;16:633–53.

[95] Klippenstein SJ, Harding LB, Glarborg P, Miller JA. The role of NNH in NO formation and control. Combust Flame 2011;158:774–89.

[96] Konnov AA, Ruyck J De. Temperature-Dependent Rate Constant for the Reaction NNH+O = NH + NO. Combust Flame 2001;1264:1258–64.

[97] Konnov AA, Dyakov I V, Ruyck JDE. Nitric Oxide Formation in Premixed Flames of H2 + CO + CO2 and Air. Proc Combust Inst 2002;29:2171–7.

[98] Konnov AA, Ruyck J De. Kinetic Modeling of the Thermal Decomposition of Ammonia. Combust Sci Technol 2000;152:23–37.

[99] Davidson DF, Kohse-Höinghaus K, Chang AY, Hanson RK. A pyrolysis mechanism for ammonia. Int J Chem Kinet 1990;22:513–35.

[100] Somarathne KDKA, Akihiro H, Hideaki K. Numerical investigation on the combustion characteristics of turbulent premixed ammonia / air flames stabilized by a swirl burner. J Fluid Sci Technol 2016;11:1–10.

[101] Somarathne KDKA, Hatakeyama S, Hayakawa A, Kobayashi H. Numerical study of a low emission gas turbine like combustor for turbulent ammonia/air premixed swirl flames with a secondary air

injection at high pressure. Int J Hydrogen Energy 2017;42:27388–99.

[102] Kurata O, Iki N, Inoue T, Matsunuma T, Tsujimura T, Furutani H. Development of a wide range-operable , rich-lean low-NOx combustor for NH3 fuel gas-turbine power generation. Proc Combust Inst 2019;37:4587–95.

[103] Somarathne KDKA, C. Okafor E, Hayakawa A, Kudo T, Kurata O, Iki N, et al. Emission characteristics of turbulent non-premixed ammonia/air and methane/air swirl flames through a rich-lean combustor under various wall thermal boundary conditions at high pressure. Combust Flame 2019;210:247–61.

[104] Rocha RC, Costa M, Bai XS. Combustion and Emission Characteristics of Ammonia under Conditions Relevant to Modern Gas Turbines. Combust Sci Technol 2020;00:1–20.

[105] Mashruk S, Xiao H, Valera-Medina A. Rich-Quench-Lean model comparison for the clean use of humidified ammonia/hydrogen combustion systems. Int J Hydrogen Energy 2021;46:4472–84.

[106] Guteša Božo M, Mashruk S, Zitouni S, Valera-Medina A. Humidified ammonia/hydrogen RQL combustion in a trigeneration gas turbine cycle. Energy Convers Manag 2021;227:1–14.

[107] Valera-Medina A, Marsh R, Runyon J, Pugh D, Beasley P, Hughes T, et al. Ammonia–methane combustion in tangential swirl burners for gas turbine power generation. Appl Energy 2017;185:1362–71.

[108] Xiao H, Valera-medina A, Bowen PJ. Study on premixed combustion characteristics of co-firing ammonia / methane fuels. Energy 2017;140:125–35.

[109] Xiao H, Valera-medina A, Marsh R, Bowen PJ. Numerical study assessing various ammonia/methane reaction models for use under gas turbine conditions. Fuel 2017;196:344–51.

[110] Somarathne KDKA, Okafor EC, Sugawara D, Hayakawa A, Kobayashi H. Effects of OH concentration and temperature on NO emission characteristics of turbulent non-premixed CH4/NH3/air flames in a two-stage gas turbine like combustor at high pressure. Proc Combust Inst 2020;000:1–8.

[111] Okafor EC, Somarathne KDKA, Ratthanan R, Hayakawa A, Kudo T, Kurata O, et al. Control of NOx and other emissions in micro gas turbine combustors fuelled with mixtures of methane and ammonia. Combust Flame 2020;211:406–16.

[112] Valera-Medina A, Pugh DG, Marsh P, Bulat G, Bowen P. Preliminary study on lean premixed combustion of ammonia-hydrogen for swirling gas turbine combustors. Int J Hydrogen Energy 2017;42:24495–503.

[113] Valera-Medina A, Gutesa M, Xiao H, Pugh D, Giles A, Goktepe B, et al. Premixed ammonia / hydrogen swirl combustion under rich fuel conditions for gas turbines operation. Int J Hydrogen Energy 2019;44:8615–26.

[114] Pugh D, Bowen P, Valera-Medina A, Giles A, Runyon J, Marsh R. Influence of steam addition and elevated ambient conditions on NOx reduction in a staged premixed swirling NH3/H2 flame. Proc Combust Inst 2019;37:5401–9.

[115] Pugh D, Bowen P, Valera-Medina A, Giles A, Runyon J, Marsh R. Influence of steam addition and elevated ambient conditions on NO x reduction in a staged premixed swirling NH 3 /H 2 flame. Proc Combust Inst 2019;37:5401–9.

[116] Gute M, Vigueras-zuniga MO, Bu M, Seljak T. Fuel rich ammonia-hydrogen injection for humidified gas turbines. Appl Energy 2019;251:113334.

[117] Hussein NA, Valera-Medina A, Alsaegh AS. Ammonia- hydrogen combustion in a swirl burner with reduction of NOx emissions. Energy Procedia 2019;158:2305–10.

[118] Pugh D, Runyon J, Bowen P, Giles A, Valera-Medina A, Marsh R, et al. An investigation of ammonia primary flame combustor concepts for emissions reduction with OH*, NH2* and NH* chemiluminescence at elevated conditions. Proc Combust Inst 2020;000:1–9.

[119] Franco MC, Rocha RC, Costa M, Yehia M. Characteristics of NH3/H2/air flames in a combustor fired by a swirl and bluff-body stabilized burner. Proc Combust Inst 2020;000:1–10.

[120] Zhu X, Khateeb AA, Guiberti TF, Roberts WL. NO and OH* emission

1102 characteristics of very-lean to stoichiometric ammonia-hydrogen-air swirl
1103 flames. Proc Combust Inst 2020;000:1–8.
1104
1105